

Optimization and Analysis of the Effects of Temperature, pH, and Injection Techniques
on a Slow-Release Permanganate Gel for DNAPL Remediation

A thesis presented to
the faculty of
the College of Arts and Sciences of Ohio University

In partial fulfillment
of the requirements for the degree
Master of Science

Rex M. Cosgrove

August 2020

© 2020 Rex M. Cosgrove. All Rights Reserved.

This thesis titled
Optimization and Analysis of the Effects of Temperature, pH, and Injection Techniques
on a Slow-Release Permanganate Gel for DNAPL Remediation

by

REX M. COSGROVE

has been approved for
the Department of Geological Sciences
and the College of Arts and Sciences by

Eung Seok Lee

Associate Professor of Geological Sciences

Florenz Plassmann

Dean, College of Arts and Sciences

ABSTRACT

COSGROVE, REX M., M.S., August 2020, Geological Sciences

Optimization and Analysis of the Effects of Temperature, pH, and Injection Techniques on a Slow-Release Permanganate Gel for DNAPL Remediation

Director of Thesis: Eung Seok Lee

This study sought to respond to the remediation challenged posed by trichloroethylene (TCE) by extending the gelation time and oxidant release duration of a slow-release permanganate gel (SRP-G). An SRP-G with these qualities would be well-suited to target TCE plumes in aquifers by spreading in the same direction as the TCE and continuing to treat the contamination over a long period. To this end, three hypotheses were tested: (A) low temperatures increase gelation time in saturated soils, (B) high pH increases gelation time in batch tests, and (C) injection of KMnO_4 into a depleted gel (repeated injection) extends release durations. In batch tests, a reduction of temperature from 23°C to 2°C increased gelation time by a median of 8 hours and a maximum of 23 hours. The sol-gel with that longest gelation time was the test with the most basic pH, however, relation between pH and gelation time was not consistent. Reinjection tests were not performed due to inability to form robust gels in saturated sands with flow. Sol-gel injection into dry sands yielded release durations of at least 1.7 days and 0.75 days in column and flow-tank, respectively.

ACKNOWLEDGMENTS

Thank you first to my advisor, Dr. Eung Seok Lee, for the chance to make a healthier future possible for communities affected by industrial contamination. He kept me focused on moving forward when the challenges of research tried to pull me in myriad directions. Thanks to my committee – Dr. Gregory Springer, Dr. Katherine Fornash, as well as Dr. Gregory Nadon, a temporary member – for being willing to help.

Thank you to Dr. Dan Hembree, who reminded me of the different pathways available toward the completion of this thesis.

Thanks to Ryan Wolbert, a fellow graduate student who kept an eye on my experiments while I was away, helped ensure distilled water was always available, and who was always good company.

Finally, thank you to Mildred Trotz, my grandmother who often checked in on the progress of this thesis to encourage me to continue, and who passed shortly before its completion.

TABLE OF CONTENTS

	Page
Abstract.....	3
Acknowledgments.....	4
List of Tables	7
List of Figures	8
Chapter 1: Introduction	9
1.1 DNAPL Contamination	9
1.2 Previous Work in the Remediation of DNAPLs.....	9
1.3 Objectives and Hypotheses.....	11
Chapter 2: Background	13
2.1 DNAPLs.....	13
2.2 Trichloroethylene	15
2.3 Current Treatment of TCE Plumes	16
2.4 Oxidation of TCE.....	17
Chapter 3: Sol-Gel Processes.....	18
3.1 Colloidal Silica.....	19
3.2 Sol-Gel Gelation	20
3.3 Effects on Gelation	21
3.4 Slow-Release Mechanism.....	26
Chapter 4: Methods.....	28
4.1 Products Employed	28
4.2 Batch Testing	28
4.3 Column Testing.....	30
4.4 Flow Tank Testing	34
Chapter 5: Results and Discussion.....	37
5.1 Batch Testing	37
5.2 Column Testing.....	43
5.3 Flow Tank Testing	51
Chapter 6: Conclusion.....	55
References.....	57
Appendix A: Batch Test Data.....	61

Appendix B: Column Test Data.....	66
Appendix C: Flow Tank Test Data.....	72

LIST OF TABLES

	Page
Table 1. Comparison of flow tank data.....	51
Table 2. Comparison of release rates	53
Table A1. Warm batch test: 140 mL colloidal silica	61
Table A2. Warm batch test: 130 mL colloidal silica, 10 mL water.....	61
Table A3. Warm batch test: 120 mL colloidal silica, 20 mL water.....	61
Table A4. Warm batch test: 130 mL colloidal silica, 10 mL NaOH	62
Table A5. Warm batch test: 120 mL colloidal silica, 20 mL NaOH	62
Table A6. Chilled batch test: 140 mL colloidal silica	63
Table A7. Chilled batch test: 130 mL colloidal silica, 10 mL water	63
Table A8. Chilled batch test: 120 mL colloidal silica, 20 mL water	64
Table A9. Chilled batch test: 130 mL colloidal silica, 10 mL NaOH	64
Table A10. Chilled batch test: 120 mL colloidal silica, 20 mL NaOH	65
Table B1. 1 mL sol-gel injection: No waiting time	66
Table B2. 1 mL sol-gel injection: 2 day waiting time	67
Table B3. 40 mL injection: 26 g/L [KMnO ₄], 45 wt% colloidal silica	67
Table B4. 40 mL injection: 40 g/L [KMnO ₄], 45 wt% colloidal silica	68
Table B5. 40 mL injection: 50 g/L [KMnO ₄], 45 wt% colloidal silica	68
Table B6. 40 mL injection: 50 g/L [KMnO ₄], 50 wt% colloidal silica	69
Table B7. Reinjection test: 10 mL sol-gel, no waiting time	69
Table B8. Reinjection test: 10 mL sol-gel, 6 day waiting time	70
Table B9. Reinjection test: First 10 mL KMnO ₄ solution	70
Table B10. Reinjection test: Second 10 mL KMnO ₄ solution.....	71
Table C1. Flow tank test: First row	72
Table C2. Flow tank test: Second row	72
Table C3. Flow tank test: Third row.....	72
Table C4. Flow tank test: Fourth row	73

LIST OF FIGURES

	Page
Figure 1. Diagram of a DNAPL spill.....	14
Figure 2. Structure of a TCE molecule	15
Figure 3. Structure of a colloidal silica particle	20
Figure 4. Transmission electron microscope images of silica gel	22
Figure 5. Hypothetical relation between pH and gelation time	25
Figure 6. Relation between temperature and gelation time	26
Figure 7. Viscotester	30
Figure 8. Low-angle column testing setup.....	32
Figure 9. Vertical column testing setup	34
Figure 10. Diagram of the flow tank.....	35
Figure 11. Room temperature batch test.....	39
Figure 12. Chilled batch test	41
Figure 13. Pramik (2017) batch tests	43
Figure 14. Small injection column test	44
Figure 15. Varying concentration column test	46
Figure 16. Reinjection column test.....	48
Figure 17. Dry sand column test.....	49
Figure 18. Dry sand column photo	51
Figure B1. Absorbance to KMnO_4 Concentration	66

CHAPTER 1: INTRODUCTION

1.1 DNAPL Contamination

Dense non-aqueous phase liquid (DNAPL) contamination is a common problem in world groundwater supplies. Clean-up efforts are hindered by the unpredictable spread of the contamination through heterogeneous aquifers, which is worsened by the DNAPL's low solubility, which permits it to continue dissolving into groundwater for long periods (Mercer & Cohen, 1990). The Interstate Technology Regulatory Council (2012) considers it optimistic to plan for DNAPL contaminated sites to achieve remediation with a generation-long project (which they define as 20 years). In order to meet even that long timescale, a variety of remediation techniques need to be applied in plans tailored to each site.

The slow-release permanganate gel remediation (SRP-G) scheme proposed here will deal with trichloroethylene (TCE). This chlorinated solvent is the most common DNAPL found in groundwater, and it presents serious health risks to those exposed to it (US EPA, 2003). A carcinogen, it presents a human health risk, capable of causing organ damage and behavioral changes (IARC, 1995; Kueper et al., 2003). Although there are several methods for remediation, they are often lengthy and expensive processes, ensuring that more of the sites will go untreated unless a more economical alternative is found.

1.2 Previous Work in the Remediation of DNAPLs

The present proposal for investigating SRP-G treatment takes its cues from existing DNAPL remediation technologies and previous studies at Ohio University

regarding SRP-G properties. It uses the same chemical remediation method as the existing flushing technique (that is, oxidation), while avoiding problems that prevent that technique from being used for disperse DNAPL plumes. Prior studies have identified potassium permanganate (KMnO_4) as an ideal chemical oxidant and colloidal silica as a gelling agent, providing a sol-gel capable of reaching widely through an aquifer.

In a slow-release gel, an oxidant, in this case KMnO_4 , is suspended in a sol-gel. This starts as an easily injectable sol, then after a period of lag time increases in viscosity until it becomes a gel from which an oxidant can be released (Lee & Schwartz, 2007b). This study represents a continuation of the work conducted by several of Dr. Eung Seok Lee's past graduate students toward the goal of producing an SRP-G that spreads widely through an aquifer before gelation and releases permanganate (MnO_4^-) for months afterward. The studies have successively improved results with an in-situ, well-based injection scheme using varying KMnO_4 solutions combined with colloidal silica gelling agents. Initial work by Olson (2011) first identified colloidal silica as the optimal gelling agent for use with potassium permanganate. Gupta (2013) recognized silica and potassium permanganate concentrations as the primary controlling factors on gelation lag time, the period lasting from injection until full gelation. The latter study further identified the KMnO_4 release rates necessary to successfully remediate varying concentrations of TCE.

Further studies sought to optimize the SRP-G to have a long gelation time and a long KMnO_4 release duration. The water flow present in real-world aquifers presented another problem, as it can cause dilution by mechanical dispersion. Hastings (2015)

suggested that KMnO_4 concentration has the greatest effect on lag time, while silica concentration more strongly affects KMnO_4 release duration. He produced a gel capable of releasing KMnO_4 for 9.2 days in porous media with flowing water. Most recently, Pramik (2017) suggested that cool temperatures also reduce the viscosity of the initial solution, which allows for a higher silica and KMnO_4 concentration without compromising injectability. Her solution reached 14.1 days of MnO_4^- release.

1.3 Objectives and Hypotheses

The purpose of this study was to produce an SRP-G treatment that can be widely dispersed through an aquifer and has a long oxidant release period. These two qualities maximize the amount of water that can be oxidized by a single treatment with the sol-gel. The previous studies by Gupta (2013), Hastings (2015), and Pramik (2017) each worked toward a more effective SRP-G using colloidal silica and KMnO_4 . This study continued to build on this past work with the goal of producing a sol-gel with a gelation time of 3 days and a release period of up to a month.

It was hypothesized that (A) low temperatures would increase gelation time in saturated soils in batch tests, that (B) high pH would increase gelation time in batch tests, and that (C) injection of KMnO_4 into a depleted gel (repeated injection) would extend release durations. Toward hypothesis A, batch tests were used to investigate the impact of low temperature on gelation time and compare with the preliminary results in Pramik (2017). Toward hypothesis B, batch tests were used to determine the optimal combination of pH and potassium permanganate concentration. Toward hypothesis C, column and small plastic flow-tank were used to determine whether a SRP-G solution injected into

sands would form gel and increase release duration, and also whether repeated injection of SRP-G into a depleted gel would further increase the release duration.

CHAPTER 2: BACKGROUND

2.1 DNAPLs

Dense non-aqueous phase liquids (DNAPLs) are low-solubility liquids that are denser than water; these two qualities make DNAPL contamination dangerous and challenging to remediate. Once introduced to an environment, they sink through soil and rock, then pool above an aquitard (Figure 1). Their low solubility ensures that this contamination is long-lasting and widespread, not significantly diluted even over long periods (Mercer & Cohen, 1980). Further, blobs of residual DNAPL are left behind in every pore through which the plume passes, held in place by capillary action (ITRC, 2012). The plume is carried by advection in the direction of water flow, is diluted by dispersion, and its distribution become practically unpredictable as it follows unknown pathways through a heterogeneous aquifer (Koch & Nowak, 2015). This combination of factors produces wide zones of contamination that cannot be eliminated with a simple, one-size-fits-all remediation plan, rather requiring a variety of methods tailored to each site's individual characteristics.

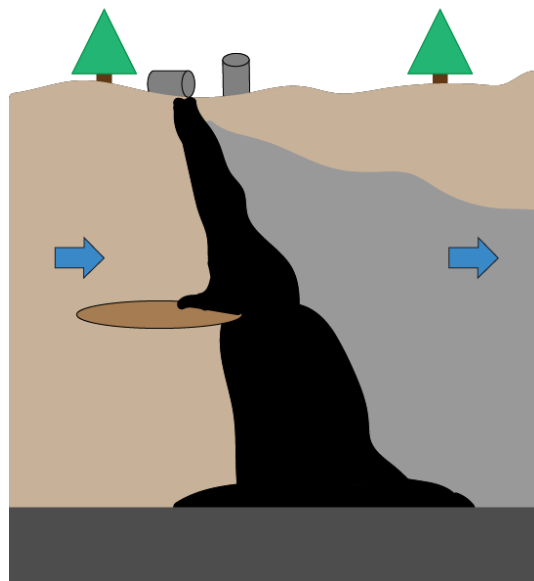


Figure 1. Schematic drawing showing the wide spread of contaminant following a DNAPL spill, in which black represents the concentrated plume that sinks through the aquifer and remains in pore spaces, while the grey represents the dilute plume that is spread through a wide area by groundwater flow (indicated by the blue arrows).

In addition to being widespread in the area around a single site, DNAPL contamination is widespread throughout the developed world. They are found at 3,000 Department of Defense sites across the U.S., and at 80% of all Superfund sites with groundwater contamination (US EPA, 1997). In 2002, 787 Superfund sites had groundwater contamination present (US EPA, 2002). Taken together, these numbers suggest some 630 DNAPL contaminated Superfund sites.

Included in this category are some pesticides, coal tar, creosotes, and, most commonly, organic solvents (US EPA, 2003). As such, it is commonly found around sites related to metal industries, in urban areas where growing populations are now demanding increased amounts of water. Additional pressures that require new attempts to remediate these sites include lack of unutilized alternative water sources and deteriorating quality in current sources, especially as a result of agricultural runoff (Rivett, 2012). In the past,

many of these sites were written off as too expensive or difficult to remediate, but the large volume of water affected across all these sites makes this stance unsustainable in the face of new demand on the public water supply.

2.2 Trichloroethylene

This study aims to develop a treatment particularly for trichloroethylene (TCE) contamination. TCE belongs to a category of compounds known as chlorinated solvents. As an ethylene-type solvent, it consists of two carbon atoms bound by a double bond and four more atoms bonded to the carbons, in this case with the formula C_2Cl_3H , as represented in figure 2 (Stroo & Ward, 2010).

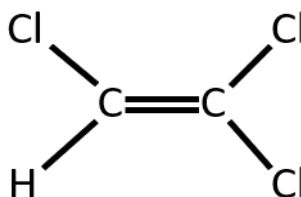


Figure 2. Chemical structure of a TCE molecule.

This organic solvent was used in industry starting in the 1930s (Rivett et al., 1990), and was only recognized as a risk to groundwater supplies in the 1970s (Pandow & Cherry, 1996). This long and widespread usage has made it the most common organic contaminant found at Superfund sites in the U.S. (US EPA, 2015). Between 9% and 34% of drinking water supply sources in the US have some TCE contamination, though most of these levels are within levels recommended by the EPA (US EPA, 2001). Present in

potentially important water sources across the country, it is a good target for new remediation techniques.

Chronic exposure to TCE causes a variety of health effects when consumed in water. It is a carcinogen, particularly promoting cancer in the liver, kidneys, and lymph nodes (US EPA, 2016). Aside from this risk, the EPA considers its most concerning effects to be those on fetal development, the kidneys, and the immune system (US EPA, 2001). Rat pups born to mothers that drank TCE-contaminated water while pregnant have malformed valves and septa in the heart, with greater risks at higher concentrations of TCE. The fetal development process affected works the same way in humans and rats, so it is expected that this result would hold in humans (Boyer et al., 2000). Further, end-stage kidney disease is more common in people exposed to TCE (Radican et al., 2006). Finally, mice exposed to 0.1 mg /mL concentrations of TCE showed reduced immune system effectiveness (Khan et al., 1995). All these concerns were enough to move the EPA to set a maximum contaminant level of 5 µg/L of TCE for U.S. drinking water (US EPA, 2001).

2.3 Current Treatment of TCE Plumes

Three technologies are widely used for the remediation of TCE: source removal, pump-and-treat, and flushing (ITRC, 2012). Source removal is perhaps the most straightforward: the most heavily contaminated area is excavated and taken elsewhere for disposal. Intuitively, this would seem to solve the problem, but in fact diffusion of TCE into unreachable areas ensure that contaminant concentration remains several orders of magnitude higher than desired for regulatory closure (Chapman & Parker, 2005).

The second remediation method, pump-and-treat requires pumping contaminated groundwater to the surface to be chemically treated, then further pumped into a body of water. Although 80% of pump-and-treat sites have achieved containment, fewer than 10% have attained regulatory closure (US EPA, 2009), and even with this questionable efficacy, it is prohibitively expensive, with annual expenses running into the low billions (Dale, 2006).

The third method, flushing, can be found on a continuum with source removal. In some cases, only a surfactant is circulated through the aquifer, which can reduce TCE's adhesion to the surrounding rock and carry the contaminant to another well to be pumped out. This technique is of doubtful utility in heterogeneous or fractured material (US EPA, 2000). More commonly, an oxidant is directly injected into the aquifer to react with TCE and produce a precipitate and a variety of ions (which depend on the oxidant used). This works for pools and small plumes, but its usefulness for larger zones of contamination is impeded by the resulting precipitate's pore-plugging, which blocks the oxidant's path to areas of contamination (Lee & Schwartz, 2007b; Lee et al., 2008). These pores represent small spaces between the grains that comprise the aquifer; the addition of a new solid where there was gas or liquid inherently blocks flow through paths that were previously open. Since the oxidant naturally reacts with TCE close to the injection site first, paths deeper into the aquifer become blocked. If this problem were solved, chemical oxidant could be used to treat much larger volumes and quantities of TCE.

2.4 Oxidation of TCE

The chemical oxidant used in this study is potassium permanganate (KMnO_4),

which has already been used prominently in other oxidation schemes (Lee et al., 2009; Lee & Schwartz, 2007a). It is therefore better understood than other potential oxidants and has established qualities that make it more useful. For instance, because of its low reaction rate, it remains in the subsurface longer than alternatives, which allows it to spread longer distances and come into contact with more contaminant (Huling & Pivetz, 2006). Its diffusion coefficient is higher than that of TCE, so it will outpace the spread of TCE in portions of the aquifer dominated by diffusive transport (Lide, 2004). It is also inexpensive and effective across a wide pH range (Yan & Schwartz, 2000).

The oxidation of TCE by KMnO_4 results in MnO_2 precipitate, carbon dioxide gas, and chloride and hydrogen ions (Lee et al., 2009). The reaction proceeds (Lee & Schwartz, 2007a):



The precipitate produced here represents the major drawback of using KMnO_4 in chemical oxidation treatment. It can block pores and prevent parts of the aquifer from being exposed to treatment (Lee et al., 2009; Lee & Schwartz, 2007a). This is not an insurmountable obstacle. Rather, it has already been shown that releasing KMnO_4 slowly via a sol-gel allows it to spread farther through sandy media (Gupta, 2013; Olsen, 2011; Hastings, 2015; Pramik, 2017). So the natural disadvantage of using KMnO_4 is negated by the use of this additional technology.

CHAPTER 3: SOL-GEL PROCESSES

3.1 Colloidal Silica

A number of slow-release delivery systems have been used in tandem with oxidants to react with and neutralize contaminants. Long release times can replace repeated treatments, retaining remediation effectiveness while requiring less labor. One study installed “candles” made of a mix of paraffin wax and KMnO_4 crystals into wells (Christenson et al., 2016), while another encased the KMnO_4 particles in a manganese oxide shell (Omoike & Harmon, 2019). Previous studies at Ohio University have identified colloidal silica as a strong candidate for a matrix material. It is nontoxic and water insoluble, while also being chemically compatible with the proven oxidant KMnO_4 and capable of releasing it into the environment at a controlled rate (Olson, 2011). The mixture of colloidal silica and KMnO_4 has a variable gelation time that can be extended by several means (Gupta, 2013). Given these advantages, recent studies have focused on optimizing silica/ KMnO_4 sol-gels for use as slow-release delivery systems (Hastings, 2013; Pramik, 2017).

Colloidal silica is a liquid suspension of amorphous silica particles, ranging in size from 10 to 10,000 angstroms, small enough to stay suspended indefinitely. Each particle is composed of silicon atoms surrounded by oxygen atoms, with hydroxyl groups at the edges (Bergna, 1994). These hydroxyl groups dissociate partly when in solution, producing a high negative charge that attracts cations and results in a double electrical layer surrounding the particles (Figure 3). The larger the negative charge on each particle, the more cations collect around them, generating strongly positive outer layers that hold

particles apart, thus preventing gelation (Siahpoosh, 2011). The effect that charges on clay may have on these outer layers is uncertain and open to new investigation.

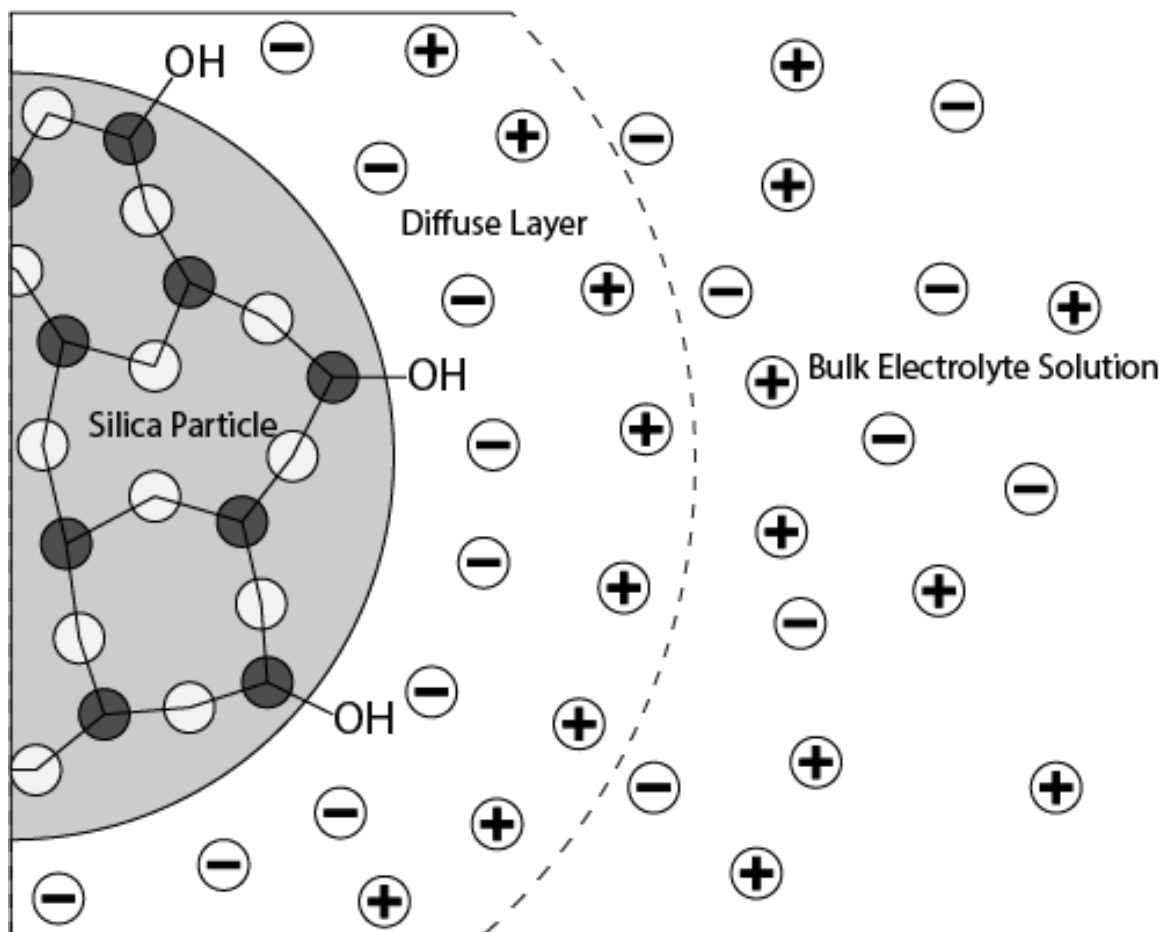


Figure 3. Schematic structure of a hydroxylated colloidal silica particle and its associated double electrical layer.

3.2 Sol-Gel Gelation

Through the process of gelation, the silica particles are organized into a framework that fills the whole volume of the sol. The resulting gel structure encloses a liquid phase (here KMnO_4) that is continuous throughout its volume. To avoid this in silica colloids produced for sale, alkaline solutions are added to the sol, which increases

the negative charge on the silica particles, resulting in a more strongly positive outer shell charge that repels other particles and prevents collisions (Iler, 1979). When gelation is desired, it can be catalyzed using an acid or a salt. When pH is very low, hydrolysis produces new hydroxyl groups that condense to form siloxane bonds, which then bond to form chains and networks (Change et al., 2015). In this case, however, KMnO_4 serves as a salt catalyst.

When a salt is added to colloidal silica, it dissolves (in this case dissociating into K^+ and MnO_4^-), and cations attach to the silica particles. The negative charge on the particles weakens, lowering their zeta potentials. More anions can penetrate the double electrical layer, including anions sourced from the salt catalyst (here MnO_4^-), and the positive surface charges that had held the particles apart begin to allow more particle collisions (Mao et al., 2014). Gelation begins. A cation is adsorbed onto a silica particle, bonding with a silanol group (Si-O-H) on its surface, then when that particle collides with another silica particle, the cation bonds with a silanol group there, linking the two particles together (Iler, 1979). As collisions between particles continue, more particles are linked, finally resulting in the gel framework.

3.3 Effects on Gelation

The process of gelation is influenced by several variables: catalyst concentration, silica concentration, silica particle size, pH, and temperature. These factors affect when gelation begins by weakening the double electric layer and affect the rate at which it proceeds by increasing or decreasing the number of collisions between particles. The structure and characteristics of the resulting gel depend on the same factors.

Salt concentration has a simple linear relation with gelation time; the more salt is added, the faster gelation proceeds (Trompette & Meireles, 2003). Higher concentrations of salt mean more cations, so the thickness of the double layer is reduced further, and gelation is more heavily favored. The gel that results is less porous the more salt is added (Figure 4), by an uncertain mechanism (Murakata et al., 1992). In this case, since KMnO_4 is used both as the catalyst and the oxidant, increasing its concentration also increases the release duration, for the simple reason that there is more oxidant to be released (Hastings, 2015). Problematically, the effect encouraging bonds among silica particles begins as soon as the KMnO_4 is added to the solution, producing a higher initial viscosity that is undesirable for achieving a wide gel dispersal.

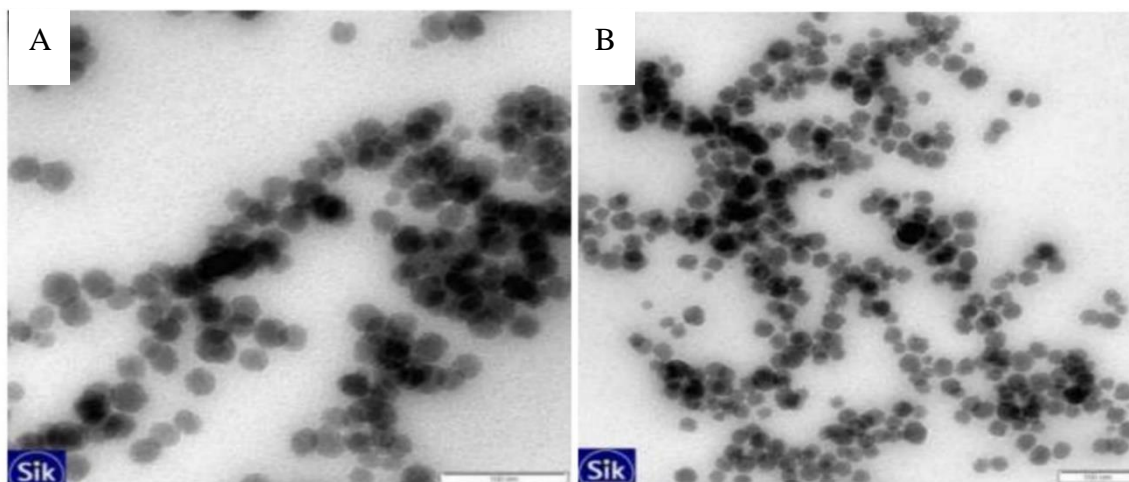


Figure 4. Transmission electron microscope images of 9 wt% silica gel. A.) has an NaCl concentration of 0.5 M, while B.) has an NaCl concentration of 0.9 M. Both have a pH of 4. B.) has a less porous structure as a result of higher salt concentrations (Siahpoosh, 2011).

Hastings (2015) gave special attention to the effect of varying silica concentrations in the sol-gel. It was found that silica concentration did not affect gelation

rates, but that higher silica concentrations did increase the duration over which KMnO_4 was released. Higher silica concentrations permit gelation with smaller amounts of catalyst and result in a stronger gel that resists diffusion and releases its KMnO_4 over a longer period.

The initial size of silica particles in the colloid also affects the gelation rate. Smaller particles have less surface area where a successful collision and reaction can take place, which reduces the gelation rate (Sögaard, 2018). This quality is hard to utilize, as it is controlled during the original production of the colloid, not after its purchase, and particle size closely correlates with silica concentration, anyway (Pramik, 2017). Also, colloids are typically advertised according to their chemistry and concentration, not the size of their particles. Nonetheless, it contributes to a full understanding of the gelation process.

The pH of a silica sol-gel has a multifaceted interplay with gelation. Above pH values of 6-7, higher pH generally leads to longer gelation times because silanol groups on the surface of the silica particle (Figure 3) dissociate, producing a more negatively charged surface. The strongly charged surfaces of the particles repel each other, preventing the collisions necessary for gelation reactions to take place. Additionally, a sol that gels at a very basic pH produces a more durable and less porous gel (Sögaard, 2018; Siahpoosh, 2011). However, below that pH range, this relationship is complicated by less straightforward forces, causing highly acidic sols to have longer gelation times, as well (Figure 5; Pedrotti et al., 2017).

The choice of base to be added to the sol-gel to affect pH adds further interactions

among factors. For instance, K^+ ions have been found to adsorb in large quantity to the surface of silica particles, which creates greater resistance to gelation. It would therefore be undesirable to add KOH to a silica sol-gel for the purpose of lowering its pH and increasing its gelation time, because the effect of OH^- ions would be diminished. By contrast, Na^+ ions do not adsorb to silica surfaces as easily, causing less interference with the effect of pH on gelation (Frank, 2002).

Problematically, high pH (>10) can cause the dissolution of silica in solution, resulting in high silicate concentrations. These silicates can deprotonate and introduce H^+ , creating a buffer effect against attempts at increasing pH (Alexander et al., 1954).

Further chemical effects of silicates in the sol-gel are possible but uncertain.

Additionally, very high pH (>11) can lead to gel dissolution when K^+ is used as a catalyst (Depasse & Wotillon, 1970).

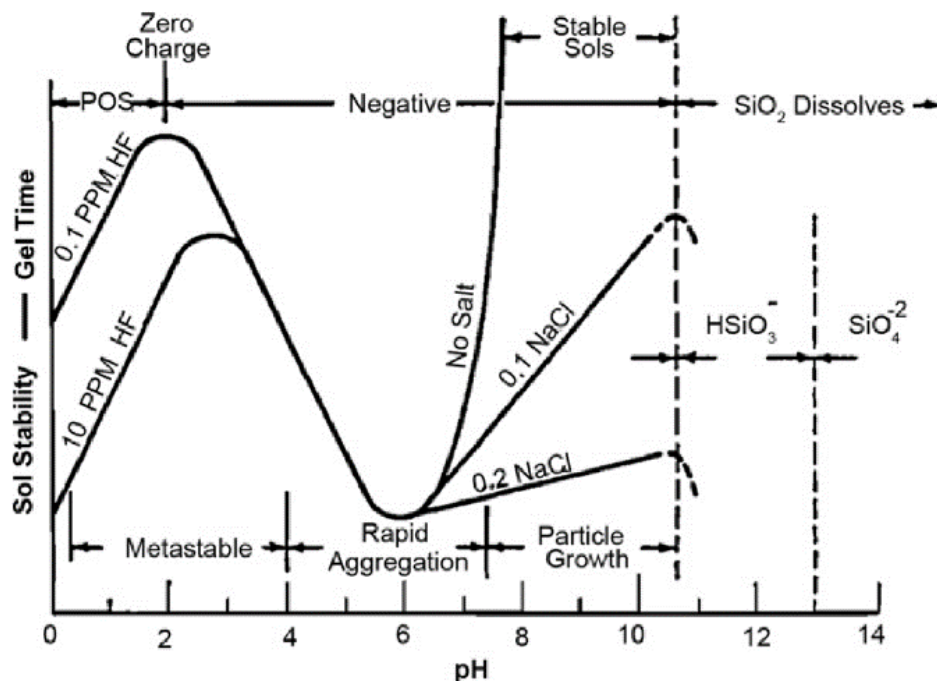


Figure 5. Gelation times are long at both high and low pH, and they are short at moderate pH (Iler, 1979).

By comparison to pH, the effect of temperature on gelation is straightforward. Lower temperatures lengthen gelation time. Less energy is available to drive reactions, and each collision between particles is less likely to succeed in creating a bond (Pramik, 2017). A silica gel formed at low temperatures will have a smaller percentage of its silica particles included in the gel framework, producing a weaker gel (Butrón et al., 2009), though this is not critical for the purposes of an SRP-G. They are related exponentially, with the longest gelation times under 10°C. By the trend in Figure 6, cooling beyond that point is expected to have only marginal effects on gelation time. Cooling beyond 0°C is likely not possible, because the silica would precipitate from the colloid below that point, and the water would freeze, according to Gregory Harris of Thermo Fisher Scientific (personal communication, March 8, 2019).

A previous study on the effects of pH and temperature on sol-gels shows a simple compounding of their effects on gelation. That is, a chilled sol-gel of low pH will have a longer gelation time than either a chilled sol-gel of moderate pH or a warm sol-gel of low pH (Shim et al., 2005). As that study was conducted on a block copolymer sol-gel with a gelation chemistry based on hydrophilic-hydrophobic interactions, that result is suggestive but not directly applicable to the silica sol-gel studied here.

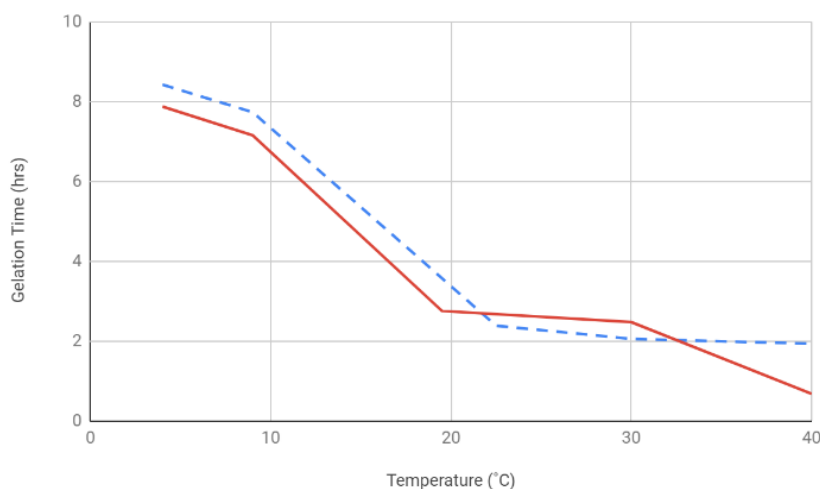


Figure 6. Relationship between temperature and gelation time, where the dashed line represents a 26 g/L [KMnO₄] sol-gel and the solid line represents a 28 g/L [KMnO₄] sol-gel (adapted from Pramik, 2017).

3.4 Slow-Release Mechanism

The sol-gel produced by these means serves as a semi-passive delivery system for KMnO₄, slowly releasing it into an aquifer to oxidize a large quantity of TCE over a long period of time. Gels, pellets, and cylinders have all been used to similar effect, but gels offer a wider range of oxidant release durations, including durations longer than those possible by other means (Lee & Schwartz, 2007a). The wide dispersion possible with a

sol-gel allows for a large volume of aquifer to be exposed to the oxidant using a single injection well, while also avoiding the problems of pore plugging and incomplete mixing between oxidant and contaminant faced by other methods (Lee et al., 2008; Lee & Schwartz, 2007a).

Once the sol is injected, it spreads widely through the aquifer until its viscosity reaches a high enough point to hold it in place. After gelation, the oxidant is slowly released into the aquifer, primarily by diffusion along the KMnO_4 concentration gradient, in response to groundwater flow (Amiri, Øye, & Sjöblom, 2009; Lee et al., 2008). The importance of diffusion in the distribution of the oxidant lends importance to the structure of the gel; a denser, less porous gel structure results in lower diffusion rates and a longer release duration (Pokusaev et al., 2018). The advantage of using a gel, however, lies in a secondary process in which the dissolution of the KMnO_4 on the outer edges of the gel creates new porosity, exposing the oxidant inside after a period of time (Keen et al., 1992). Thus, the whole volume of KMnO_4 is slowly but surely released into the aquifer.

CHAPTER 4: METHODS

4.1 Products Employed

SRP-G solutions used in this study were produced using granulated colloidal silica from Thermo Fisher Scientific and granulated KMnO_4 (99+%, ACS reagent) purchased from Acros Organics. A Bindzil 2040 and Bindzil 9950 mix had KMnO_4 added to reach the desired concentrations, then the sol was mixed with a glass rod. These products were identified in Hastings (2015) as providing the best control over gelation times. Solution pH was controlled using NaOH at 50wt% from Thermo Fisher Scientific.

4.2 Batch Testing

Small batch tests aimed to test the effect of low pH on sol-gel gelation time. In the first round of testing, two groups of sol-gels were compared; those with varying amounts of NaOH solution added (the test group), and those with equal volumes of water added, instead (the control group). Every sample had a volume of 140 mL, chosen as the minimum volume necessary to cover the viscotester rotor fully. Every sample had a KMnO_4 concentration of 26 g/L, chosen for comparison to Pramik (2017). In the test group, three batches were prepared, with a half-and-half mix of 40wt% and 50wt% colloidal silica comprising 140 mL, 130 mL, and 120 mL of the volume of each sample, and 12.43 pH NaOH solution comprising 0 mL, 10 mL, and 20 mL of the volume. In the control group, the same volumes of colloidal silica were mixed with 0 mL, 10 mL, and 20 mL of distilled water, so that pH could be tested as a variable in isolation from changes in silica concentration.

Small batch tests were conducted in two groups: one at room temperature ($\sim 23^\circ\text{C}$)

and one at 2°C. Reagents were always added in the following order: colloidal silica, KMnO_4 , NaOH . They were then mixed with a glass stirring rod. The tops of the containers were covered with plastic bags, which were held on with rubber bands. The room temperature batches were placed in the back of a fume hood where they would not be disturbed, and the chilled batches were placed in a refrigerator (where the temperature was monitored with a glass thermometer). Each container was stirred approximately once an hour, and viscosity was measured at least every other hour, except overnight (Figure 7). The Thermo Scientific viscotester included three rotors: R1, R2, and R3. R1, rated for use at viscosities between 3 and 150 dPas, was used for measurements under approximately 100 dPas (as viscosities <3 dPas are not relevant to the gelation time). R3, rated for use at viscosities between 100 and 4000 dPas, was used for measurements over approximately 100 dPas. The point where the rotor was switched was based on subjective judgment.



Figure 7. Setup used for viscosity testing, showing Thermo Scientific viscotester and one of the 140 mL containers used for all samples.

4.3 Column Testing

Column flow-through tests were carried out in glass columns 16 cm long and 4.8 cm in diameter. Coarse silica sand (sieve size = 60 – 100 mesh) was washed with deionized water, then saturated and added by small portions, ensuring no pockets of air would form. Distilled water was pumped into the columns using peristaltic pumps (Masterflex L/S, Cole-Parmer; Ismatec BV-GE); outflow from the columns was allowed to drain via gravity. For all but the last test, the columns were set at an angle of 11° . Samples of the outflow were collected by placing a 2.5 mL cuvette below the column to fill; the length of time it took to fill this cuvette was used to establish flow rates, keeping them consistent within rounds of testing where possible, and allowing for normalization

where not. MnO_4^- concentrations were tested from these samples using a UV Visible Spectrometer.

The first column test used a sol-gel with a 0.5 g/L concentration of KMnO_4 and no NaOH . 1 mL of this sol-gel was added to the column via the peristaltic pump. In the control run, distilled water was pumped through the column immediately following this injection, in order to flush the sol-gel out while it was still fluid. Samples were then taken until MnO_4^- concentration remained at zero. The test round used the same injection, but after the first sample with a measurable amount of MnO_4^- the pump was stopped and the end of the column was plugged for two days, providing time for the sol-gel to gel, though the eventual results suggest that gelation did not occur. Pumping and sampling were then restarted, continuing until water flow ended by equipment malfunction.

The second column test compared concentrations of KMnO_4 and silica concentration in the sol-gel. Each column was injected with one sol-gel out of 26 g/L, 40 g/L, and 50 g/L [KMnO_4] with 45 wt% colloidal silica sol-gels and 50 g/L KMnO_4 with 50 wt% colloidal silica. Columns were filled approximately halfway with wet sand, which was then saturated with 40 mL of sol-gel poured from a glass beaker. 18 hours were allowed for gelation, then pumping and sampling were started (Figure 8).



Figure 8. Experimental setup for the second round of column testing. Ismatec peristaltic pump is visible on the left, pumping water through five columns, one of which failed to give usable data. Latex around the edge of the bottom cap ensured a watertight seal.

The third column test targeted the practice of a repeated injection of liquid KMnO_4 into an exhausted gel framework. This test was performed in four stages. A first injection of 10 mL of 26 g/L $[\text{KMnO}_4]$ sol-gel was injected and had distilled water pumped in immediately after it. Pumping continued until measured $[\text{MnO}_4^-]$ reached zero, intentionally flushing the sol-gel out of the column before it could gel. A second injection of the same composition and volume of sol-gel was given 6 days to gel, then water was pumped through in the same fashion. This second injection was intended to form a gel framework that could be exhausted and refilled. This was followed by an injection of 10 mL of 26 g/L fluid KMnO_4 solution, without any colloidal silica, which was given a day to, hypothetically, refill the gel framework. Water was then pumped

through until the $[\text{MnO}_4^-]$ reached zero. This injection of fluid KMnO_4 solution was then repeated in the same fashion.

The final column test used a different column fill and arrangement; it was filled with dry sand, then stood vertically instead of the 11° incline used in the other tests (Figure 9). 100 mL of 26 g/L $[\text{KMnO}_4]$, 45 wt% colloidal silica sol-gel was poured directly into the dry sand, then given 5 days to gel. It was intended that water would then be pumped through the column, however, the impermeability of the gel prevented this. This was attributed to the injection of an excessive volume of SRP-G solution. For this study no additional column tests with injection of smaller volume of SRP-G solution were performed. Instead, efforts to create secondary permeability in the gelled SRP-G solution within the sandy media was taken. At first, distilled water of known volumes was allowed to sit on top of the gel-filled sand and periodically sampled and replaced. The observed lack of progress in exhausting the gel and the prohibitive level of attentiveness this required prompted a change in method; a small open channel was then carved along the side of the column to allow water flow. Water was then pumped into the top of the column and sampled from the bottom. After measuring MnO_4^- concentrations in the outflow samples and estimating release rates, the known volume of water was removed from the top of the gel-filled sands to compare the results.



Figure 9. Vertical column used in dry sand column test.

4.4 Flow Tank Testing

The flow tank used in testing was constructed from a clear plastic container with a sheet of plywood in the bottom and insulation-wrapped wire fencing separating the sandy portion from the inflow and outflow chambers. Thirteen holes were drilled into the plywood in the spacing indicated in the overhead view of Figure 10. Each of these holes held a thin wooden dowel rod, on which was taped two rubber tubes in the spacing indicated in the side view of Figure 10. The bottom ends of the tubes were covered with insulation to prevent plugging by sand. These tubes were long enough for their tops to remain accessible after sand was added, so that water could be pumped from these sampling wells into cuvettes for concentration testing. Instead of filling the 2.5 mL cuvette for each sample, as was the procedure for the column test, only 1 mL was pumped from the monitoring wells, then diluted with 1.5 mL of distilled water. This change, in addition to a slow sample pumping rate, was intended to avoid interrupting the flow regime of the tank.

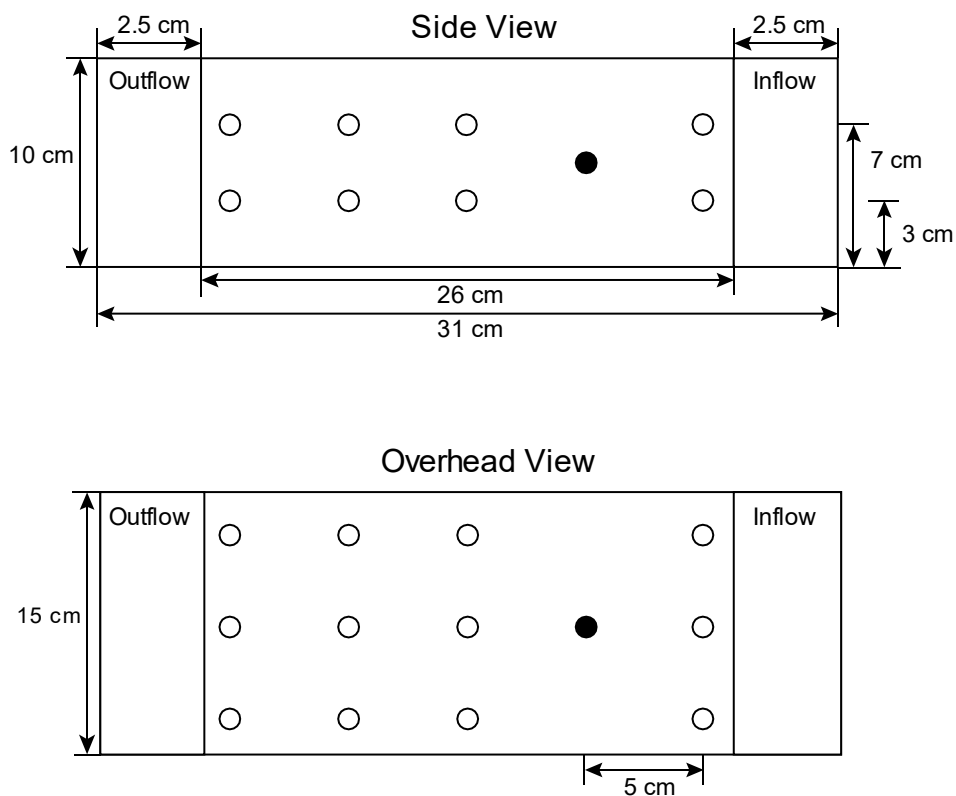


Figure 10. Diagram of the flow tank used in testing, in which the solid black circle represents the injection well and the hollow circles represent the sampling wells. Water flowed from right to left (in this diagram).

Prior to testing, dry sand was poured into the flow tank around the dowel rods holding the monitoring and injection wells to a level 1 cm below the top of the container and 2 cm above the upper monitoring wells. A sol-gel of 26 g/L $[\text{KMnO}_4]$ and 45 wt% colloidal silica was used for this test. Before any water was added to the flow tank, 40 mL of an intended 100 mL was pumped into the injection well before the pressure caused the tubing to burst at a connection point. Injection into dry sand was intended to ensure gelation, as in the dry sand column test. The flow tank was then left alone for 4 days.

Two peristaltic pumps were then put in place, one for inflow and one for outflow.

Flow through the pumps was measured and balanced at 0.11 mL/s to ensure continuous flow. Inflow was started, while the outflow tube was placed at a level with the top surface of the sand, ensuring the sand would be saturated fully. Samples were then taken from each well as was deemed necessary by the researcher.

CHAPTER 5: RESULTS AND DISCUSSION

5.1 Batch Testing

The relationship between pH and gelation time was unclear in the room temperature batch tests. The control tests (Figure 11, A) showed an expected relationship between dilution and gelation time; with 0 mL and 10 mL of distilled water added, gelation (defined as reaching 20,000 cP) occurred in 6 hours, while with 20 mL of distilled water, it took 8 hours. However, the test group (Figure 11, B) showed no change in gelation time regardless of how much NaOH solution was added; all three batches, with 0 mL (pH 9.36), 10 mL (pH 9.40), and 20 mL (pH 9.44) of NaOH solution added, gelled in 6 hours. Change in gelation time was no more than 30 minutes, making it difficult to observe the change. Experimentation with a wider pH range is recommended to test for larger changes in gelation time that would be more evident even at room temperature.

This is difficult to account for, as the gelation time would be expected to follow the trend produced by dilution, as seen in the control tests, even if pH had no effect. Instead, 20 mL of distilled water added to the sol-gel had a greater effect on gelation time than 20 mL of NaOH solution, even though they diluted the colloidal silica the same amount. It is suggested that the shorter duration of the reaction at room temperature makes small changes in gelation time hard to observe.

Additionally, although the gels with added NaOH were measured to have a maximum viscosity of around 60,000 cP compared to a maximum viscosity of less than 40,000 cP in the gels with only distilled water added (Figure 11), this is suggested to be

due to an artifact of the data collection method, rather than a real difference in texture among the different gels. The viscometer used in these tests measured viscosity by spinning a rotor in the sample, so when the sol-gels are well-gelled, shear thinning prevents the collection of accurate results. As such, the drop in measured viscosity visible as the last datapoint in each series represents a change in the sol-gel's behavior from fluid to solid, after which the rotor spins through open air in a void surrounded by gel.

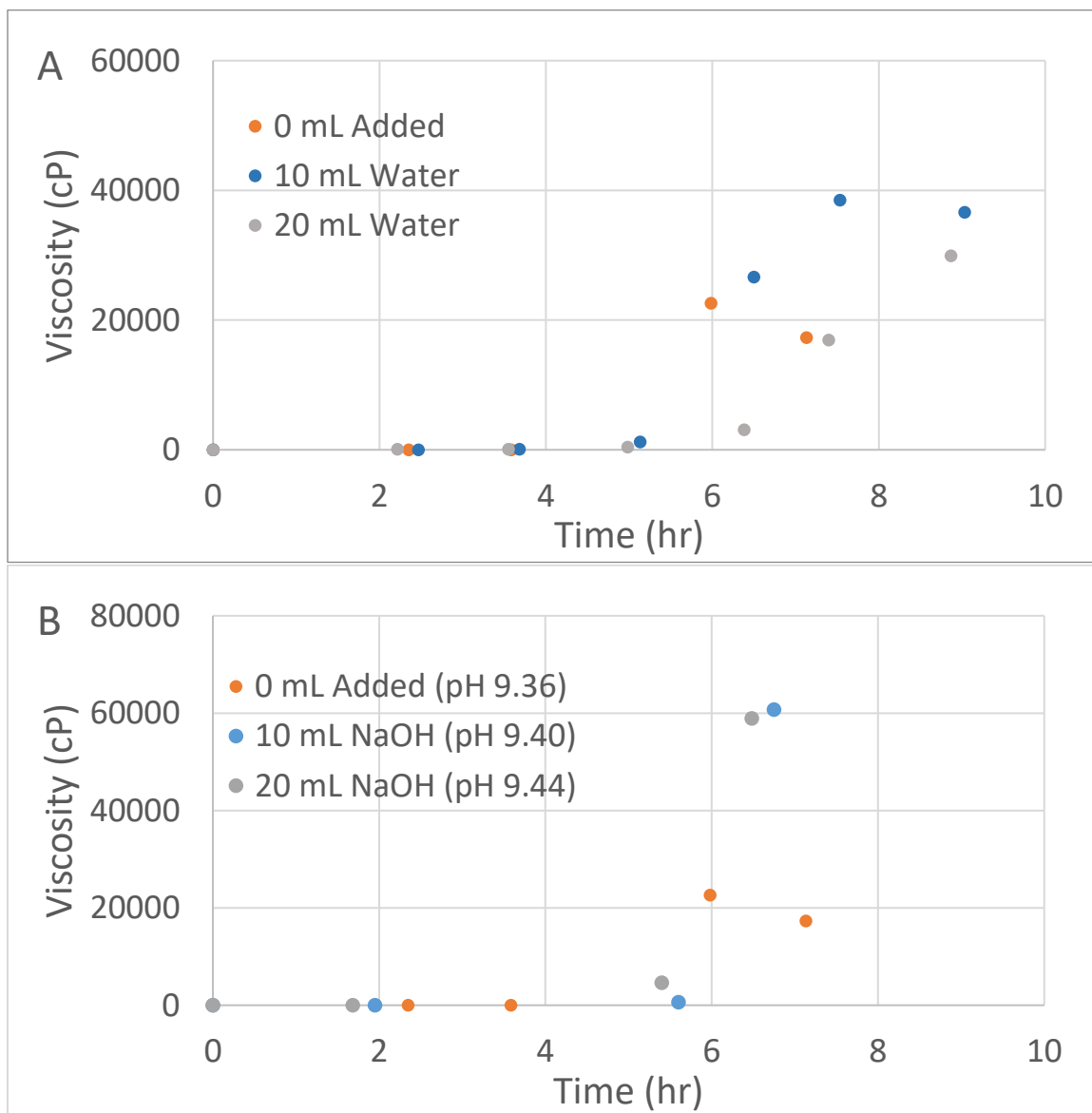


Figure 11. Room temperature ($\sim 23^{\circ}\text{C}$) batch test results. (A) was conducted at room temperature ($\sim 23^{\circ}\text{C}$) with 0, 10, and 20 mL of distilled water added as a control. (B) was conducted at room temperature with 0, 10, and 20 mL of NaOH solution added to increase pH.

All chilled batched tests had a longer gelation time than their respective room temperature tests. In the control group, the gelation time of the sol-gel with no added distilled water increased from 6 to 11 hours, that with 10 mL increased from 6 hours to 14 hours, and that with 20 mL increased from 8 hours to 20 hours. In the experimental

group, the gelation time of the sol-gel with 10 mL of added NaOH solution (pH 9.40) increased from 6 hours to 10 hours and that of the sol-gel with 20 mL of added NaOH solution (pH 9.44) increased from 6 hours to 29 hours. This is the clearest trend in testing and affirms the findings of Pramik (2017).

However, the effect of change in pH during batch testing remains inconclusive. The longest gelation time achieved, 29 hours, was in the chilled sol-gel with the most basic pH (Figure 12, B), representing a leap in gelation time rather than a consistent trend. By contrast, the gelation time of the chilled sol-gel with pH 9.40 was shorter than the gelation time of the room temperature batch with the corresponding volume of water added; the control sample gelled in 14 hours (Figure 12, A), while the test sample gelled in less than 10 hours (Figure 12, B). The lack of trend in the room temperature tests was discussed above. The long gelation time observed in the low pH, low temperature sol-gel batch suggests that the combination of pH and temperature effects merits further investigation to more fully characterize its effects. In particular, the testing of a wider pH range may establish a trend that was not observable within the range tested here.

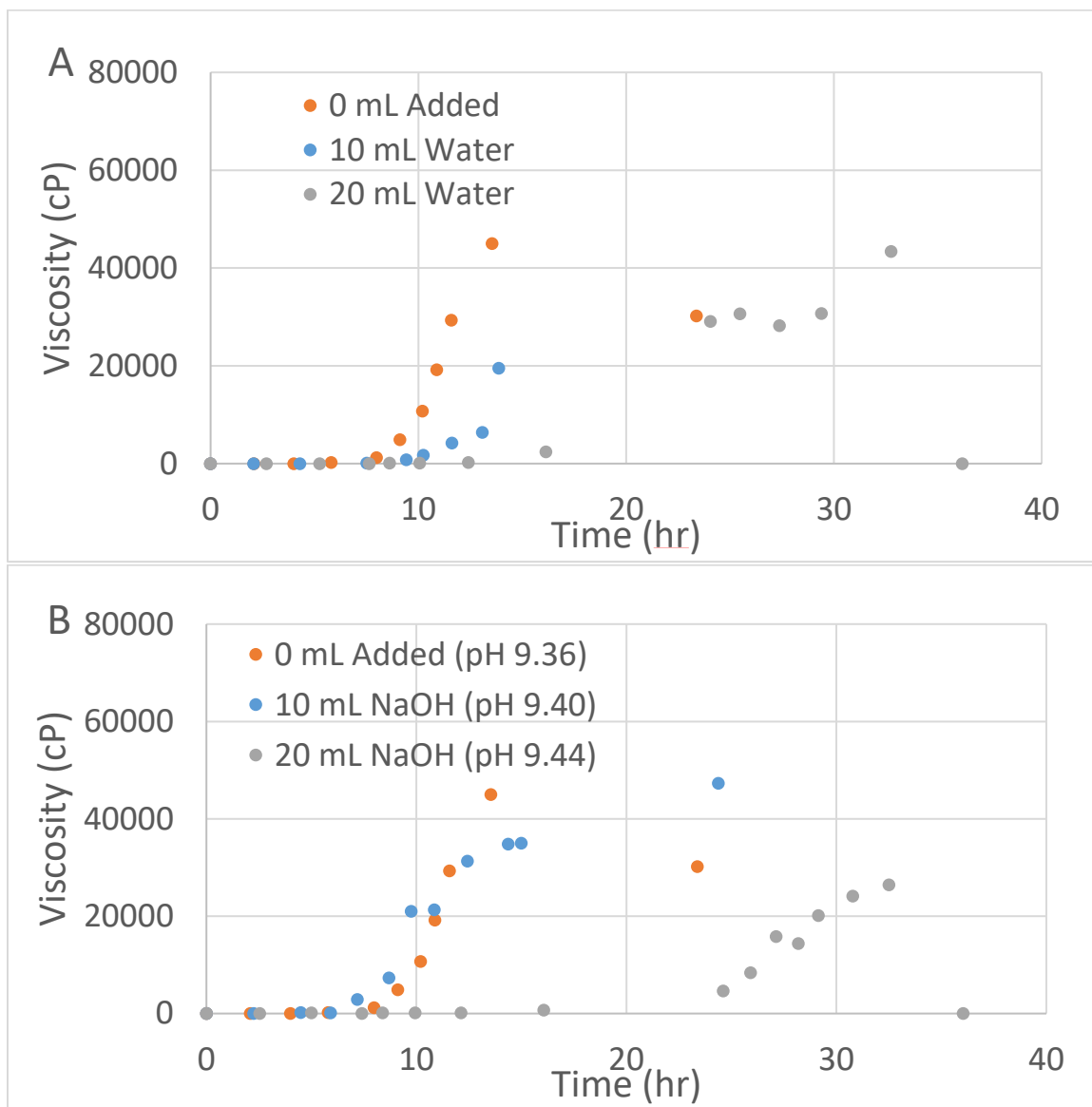


Figure 12. Chilled (2°C) batch tests. (C) was conducted at 2°C with 0, 10, and 20 mL of distilled water added as a control. (D) was conducted at 2°C with 0, 10, and 20 mL of NaOH solution added to increase pH.

In comparison to data from Pramik (2017), the batch tests in this study had slightly longer gelation times at all temperatures. In the room temperature tests, the sol-gel used in this study reached 20,000 cP at 6 hours (Figure 11), while in Pramik (2017), the room temperature test passed that mark at only 2 hours (Figure 13). Here, the chilled

2°C sol-gel with no water or KMnO_4 added (Figure 12), reached 20,000 cP at 11 hours (Figure 12), while in Pramik (2017), the 4°C batch test reached 20,000 cP at 8.5 hours (Figure 13). Although this study's 2°C test produced a 3.5 hour longer gelation time than the 4°C test in the prior study, the difference is not attributed to the effect of temperature. This is evident from the similar 4-hour difference in gelation time at room temperature. Rather, the difference stems from a slight difference in methodology. In this study, the beakers were covered over with a film of plastic held tight by a rubber band; such a practice is not mentioned in Pramik (2017). This was intended to prevent floating particles pushed through the air by air conditioning from settling in the gel and affecting the gelation process. It may be that impurities of this sort shortened the gelation time in Pramik (2017) by providing nucleation points for gel to form. Alternatively, if atmosphere exposure is necessary for the gelation reaction (the stoichiometry of which is uncertain), this may have extended the gelation times observed in this study. A combination of both factors is likely.

Both of these experimental designs have certain affinities with a real-world aquifer environment. The chemistry of groundwater can vary widely, and it is impossible to avoid impurities in the gelation process, as the current study sought to do by covering the beakers. Possible impact by gaseous atmospheric components warrants further study to determine its effect or lack thereof. Therefore, although the gelation times observed in the two studies batch tests differ, it is regarded as more important that the relation between temperature and gelation time within each study is consistent; lower temperatures result in longer gelation times.

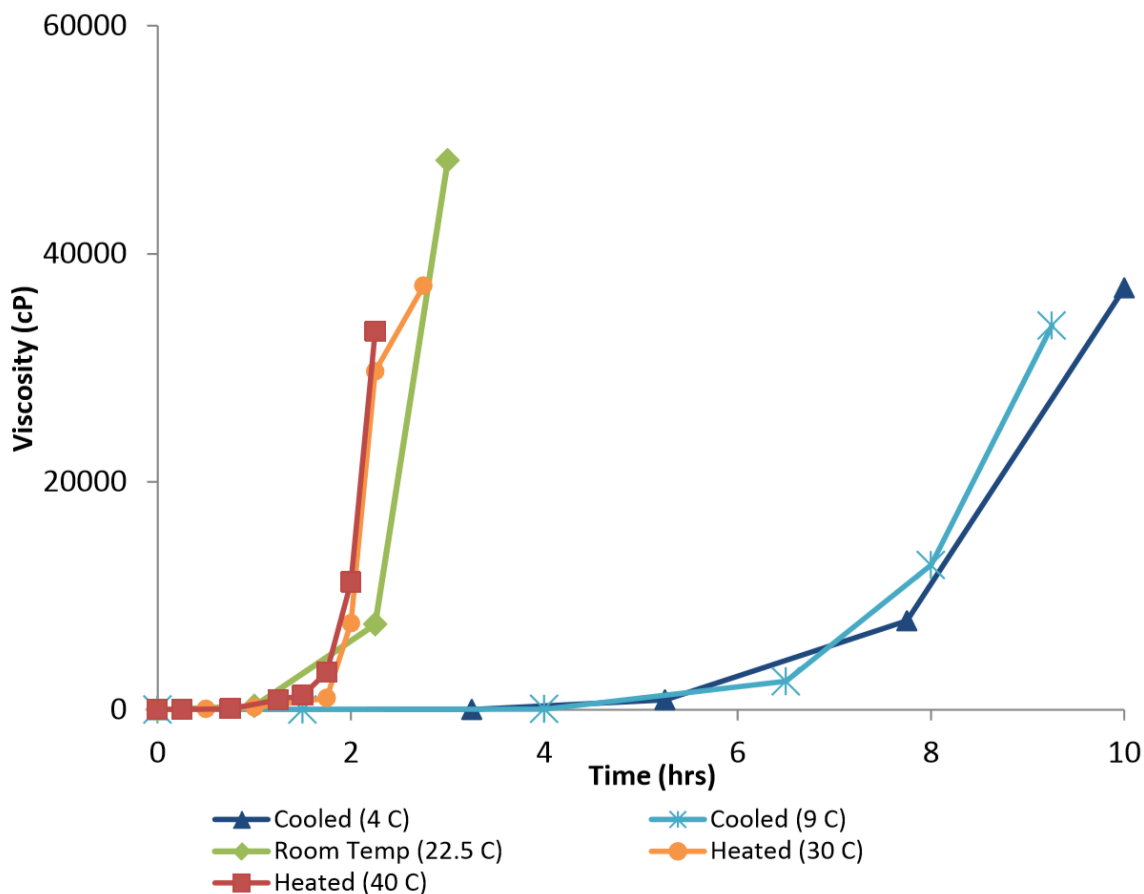


Figure 13. Viscosity over time at a range of temperatures from Pramik (2017). These batch tests used the same KMnO_4 concentration (26 g/L), temperature protocol, and viscotester as the current study, making them comparable.

5.2 Column Testing

During the first column test, the sol-gel was injected, then water pumped through the column immediately and continuously. The MnO_4^- concentration spiked to 0.11 g/L as advection brought the plume of sol-gel to the end of the column, then quickly fell to zero (Figure 14). When another sol-gel injection was followed by a two-day waiting period to allow gelation before it was pumped through the column, the peak was muted, reaching 0.02 g/L. From the data that were collected, it appears that a low level of MnO_4^- continued to be released beyond the period that release occurred without a two-day

waiting period for gelation. Observation was made through minute 400 when water stopped flowing through the column.

The muted peak and long tail in this case compared to the simple injection without the waiting period (Figure 14) suggests the formation of gel in the column during the two-day wait period. Due to the short monitoring period, the long-term release nature of the gel was not assessed. However, continuous release of low concentration of MnO_4^- in spite of the small volume of sol-gel used in this test (1 mL) represents good evidence of slow-release from the gel.

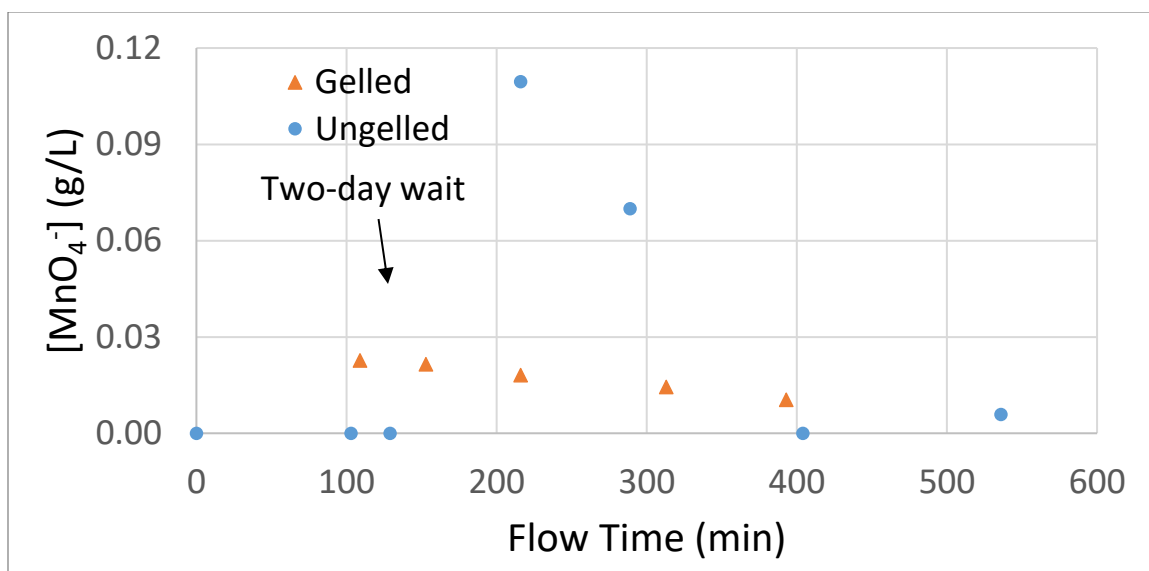


Figure 14. MnO_4^- concentration following injection of sol-gel. 1 mL of 26 g/L $[\text{KMnO}_4]$ and 45 wt% colloidal silica sol-gel was injected into a small glass column. Water was then pumped through by the same system and samples were collected on the opposite end.

The next round of column testing compared varying concentrations of KMnO_4 in the sol-gels. Since increased KMnO_4 concentration is known to reduce gelation time (Hastings, 2015; Pramik, 2017), it was thought that this would ensure gelation. The

varying combinations of colloidal silica and KMnO_4 concentrations used, as well as their respective MnO_4^- release durations are represented in Figure 15. Columns were filled approximately halfway with wet sand, which was then saturated with 40 mL of sol-gel. 18 hours were allowed for gelation. The sample with the highest silica concentration (50 wt%) is the noted outlier of the group, showing a second concentration peak (Figure 15). This peak in concentration measured at 1500 mL of water flow through the column is the result of turning the column to check for gelation. Gelation being more difficult to observe in columns than in batch tests, each column was turned once to see whether the sand would shift with the column or stay in place. Each of the columns was turned in the same manner at the same time, so if gelation were the same in all four, the same peak would have been observed. On this occasion, the 50 g/L and 45 wt% sample was judged to be the most gelled, as the sand did not shift when turned. In retrospect, this same effect could have been caused by that column being slightly drier than the others, a quality which was not recorded.

While each of the sol-gels started by releasing similar concentrations of MnO_4^- , all three of the sol-gels that used 45 wt% colloidal silica had reached zero $[\text{MnO}_4^-]$ by the 2000 mL mark, the 50 wt% sol-gel showed continued release after 5000 mL of water had passed (Figure 15). This finding accords with Hastings (2015), who suggested the higher initial silica concentration results in a tighter gel framework that is more resistant to the diffusion of its contents.

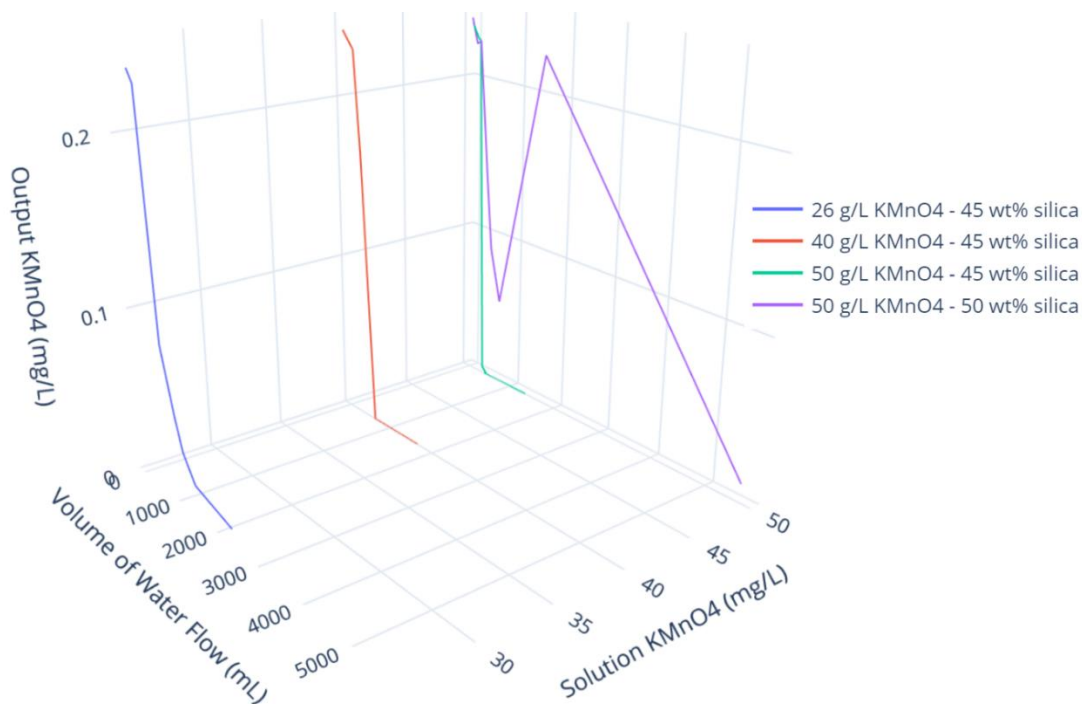


Figure 15. Column tests were conducted using sol-gels with 26 g/L, 40 g/L, and 50 g/L [KMnO₄] and 45 wt% colloidal silica and with 50 g/L KMnO₄ and 50 wt% colloidal silica. The water flow rate could not be matched perfectly among the columns, so results are displayed as a function of volume of water, for better comparison.

Reinjection tests began with an injection of 40 mL of 26 g/L [KMnO₄] that was immediately followed by distilled water. This control test, intended to pass through the column without gelation, is distinct in Figure 16 because of its later MnO₄⁻ concentration peak, reaching 0.050 g/L at 15 minutes and 0.052 g/L after 21 minutes. The second sol-gel injection was intended to gel and create a gel framework that could be refilled by injection of KMnO₄. This sol-gel had the same volume and composition as the first, but pumping of distilled water through the column did not begin until 6 days after the injection. MnO₄⁻ concentration was first measured at 0.055 g/L after 15 minutes and again at 0.055 g/L after 43 minutes. This immediate peak reflects the diffusion that took place

during the 6 days allowed for gelation. Concentration fell quickly in both cases, with the first sol-gel reaching 0.02 g/L $[\text{MnO}_4^-]$ at 307 minutes and the second sol-gel reaching 0.001 g/L $[\text{MnO}_4^-]$ at 277 minutes. The two following injections were of 26 g/L KMnO_4 dissolved in water. Both reached 0.00 g/L $[\text{MnO}_4^-]$ around the hundred-minute mark, demonstrating no extended release duration.

The close correlation between both of the sol-gel concentration curves, as outlined above, despite the expectation that only the second would form a slow-release gel, suggests that either both formed a gel or neither did. In either case, gel may have been present was not robust nor stable enough to be used in the reinjection scheme.

This result seemingly contradicts three previous studies (Gupta, 2013; Hastings, 2015; Pramik, 2017). Gupta (2013) does not state the volume of sol-gel injected into the saturated sands columns used, which may allow for diffusion of a too-small volume of sol-gel to be identified as the factor preventing gelation. As a counterpoint, Hastings (2015) used a similar volume of sol-gel in column testing (50 mL there versus the 40 mL used in the reinjection column test here), and even achieved gelation at a $[\text{KMnO}_4]$ of 20 g/L in a similar, if not identical, colloidal silica. However, that study pumped tap water through the column instead of distilled water, and the resultant impurities might encourage gelation. Additionally, Pramik (2017) showed convincing evidence of gelation in a small-scale flow tank, an environment more diffusive than a flow column. That test had a slightly higher concentration of KMnO_4 (28 g/L versus 26 g/L), but this would not seem decisive in light of Hastings (2015). However, that flow tank test did use a larger volume of sol-gel (80 mL) than any saturated sandy media test in this study. Therefore, it

appears that the diffusion of injected sol-gel leading to a failure of gelation may be countered by the injection of a sufficiently large volume of sol-gel to create an area of high concentration that persists long enough for gelation to occur.

After the lack of robust and stable gel formation seen in the reinjection test, the tested environment was switched from saturated sand to dry sand because experimentation with new mixing ratios and volumes was beyond the scope of this thesis. Although dry sand is a less realistic environment, it permits the study of a successfully formed gel, which allows conclusions to be drawn that will still apply to future studies that may find a mixing ratio that will successfully gel in saturated environments.

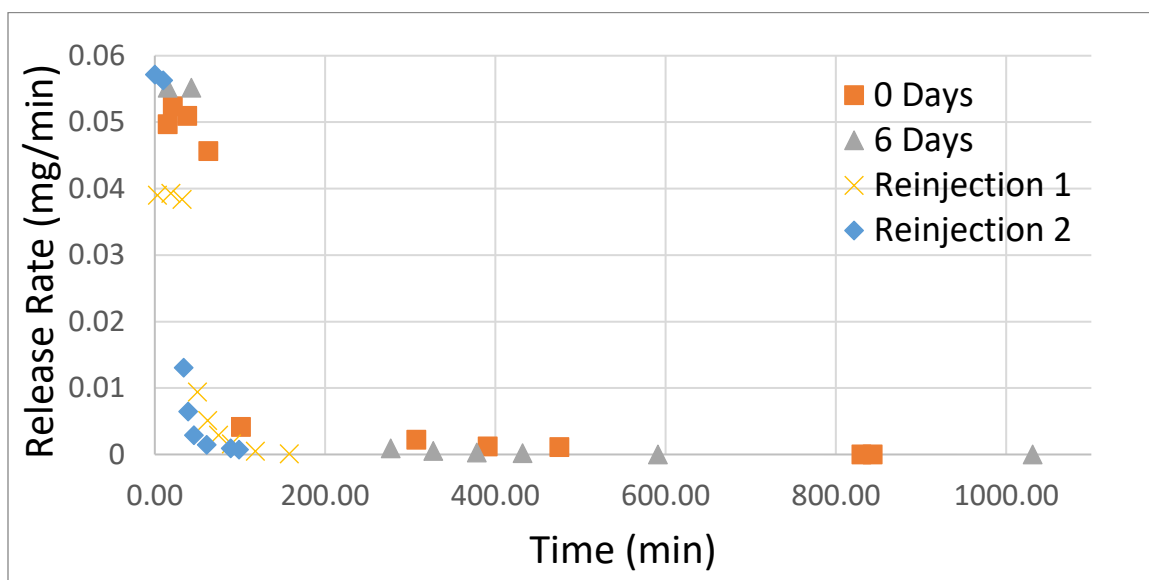


Figure 16. Results of reinjection tests, in which sol-gel was injected twice into a sand column and pumped through, in one instance with no time allowed for gelation and in the other with 6 days. Two reinjection tests were intended to refill a gel framework left behind by the second sol-gel injection.

The final column test used dry sand that was then saturated with sol-gel solution to ensure gelation. After a five-day gelation period, it was found that the gel created in

the dry sands was impermeable to water. This confirms that the formation of robust and stable gel in porous sandy media with the sol-gel solution is possible and the lack of gel stability in saturated sands was due to dilution of pore water. To test the release duration of the gel, water was initially poured on top of the column and allowed to sit, then sampled and replaced because the release of some permanganate will make gel more permeable and eventually allow for pumping. However, after a day of this manual method, little change in permanganate concentration was seen, suggesting that the time needed to make the column permeable would be prohibitively long (Figure 17). A small open channel was then carved along the side of the column to allow water flow (Figure 18).

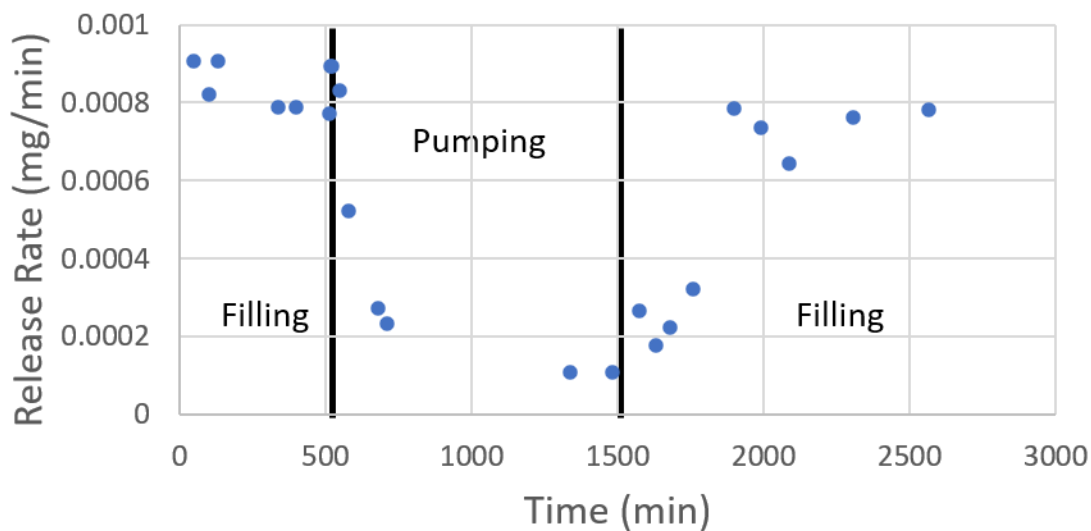


Figure 17. Showing three phases of testing the dry sand column, in which water was initially baled manually, then pumped through a channel, then once again baled, after the $[\text{MnO}_4^-]$ concentration fell very low.

The pumping phase of the test saw a rapid fall in permanganate release rate

(Figure 17). The permanganate in the loose sand produced by the carving of the channel was quickly exhausted, then the permanganate immediately surrounding the channel was, too, as observed by the coloration pattern in Figure 18. At the time, the low concentrations at the end of the pumping period generated concern that data would be impacted by measurement error, so pumping was ended, and manual filling began again. The renewed manual filling of the column resulted in an increase of permanganate release rate to initial levels (Figure 17). This demonstrates that even once the edges of the gel are exhausted, permanganate from deeper within the gel can still be released. While observation from this test was mainly qualitative and limited due to the slow release and increase in hydraulic conductivity of the gel, it also suggested that lack of gelation in previous tests is caused not by the sandy media but by dilution with water. Therefore, future trials with larger amounts of sol-gel solution with higher KMnO_4 concentration should be successful in achieving gelation.



Figure 18. The open channel where water was pumped through the column. Areas where permanganate has been depleted are clearly marked by the presence of white sand. Unseen at the top of the column is solid layer of glassy gel indicative of the solidity obtained after gelation in the absence of water.

5.3 Flow Tank Testing

Table 1. Comparison of the characteristics of flow tank data from this study and from Pramik (2017). Advection point distance is estimated using $[\text{MnO}_4^-] > 10 \text{ mg/L}$ as a cutoff. Numbers used for Pramik (2017) are taken from that study, accepting some ambiguity in the width of sandy media.

	Cosgrove (2020)	Pramik (2017)
Plume Width (cm)	13	18
Flow Rate (mL/min)	6.8	4.5
Porosity	0.3	0.25
Linear Velocity (m/day)	2.51	0.213
Advection Pt. Distance (cm)	209	25

A small flow tank test was conducted in an attempt to map the spread of

permanganate in an aquifer environment. As in the last column test, the sol-gel was injected into dry sand to ensure gelation. Based on findings from last column test, injection of sol-gel into dry sands would reliably create gel in the porous media. After allowing 12 days of gelation time, deionized water was flown through the sands using the input and output chambers constructed in the flow tank. Ambient flow rate of 6.8 mL/min was maintained using peristaltic pumps. Once the sandy media has been saturated with deionized water, water samples were collected from the multi-level sampling wells at different locations and depths to monitor 3-dimensional distribution of MnO_4^- plume created by the release from the gelled SRP-G solution.

The peak $[\text{MnO}_4^-]$ measured was 0.584 g/L at the well 5 cm straight downstream from the injection point at 2 hours and 20 minutes into pumping and 2 minutes following the saturation of the sand in the tank. This was the first sample taken, and this accords with the simple fact that there had not yet been time for much movement to take place. This is higher than the maximum concentration measured in Pramik (2017), which was 0.240 g/L, despite the injection of twice the volume of sol-gel in the earlier study, likely as a result of difference in method. The sol-gel used in that study's flow tank was injected into saturated material, allowing it to immediately spread through the tank. By contrast, the sol-gel in this study remained very concentrated close to its injection site until water was introduced after gelation, even creating enough pressure to pop the tubing off the injection well prematurely.

Using 10 mg/L as a cutoff, the last MnO_4^- detected was at 19 hours after saturation and 21 hours after the start of pumping. The monitoring well was 15 cm

downstream from the injection well. As the pumping rate (Q) in flow tank was 6.8 mL/min, the cross-sectional area (A) of saturated sand in the tank was 130 cm², and the porosity (n_e) of clean sand is estimated at 0.3, the linear flow velocity ($v = Q/(A*n_e)$) can be calculated as 0.174 cm/min, or 2.51 m/day. An advection point travelling from the injection well over 19 hours would have travelled 199 cm, so the fact that any MnO₄⁻ remained 15 cm from the injection well after that period suggests a prolonged release duration due to gel formation and delayed release of MnO₄⁻ from the gel. Taking 199 cm as the advection point of a plume and 15 cm as the back edge, this suggests a 184 cm long plume in rough estimation of advective transport without consideration of longitudinal dispersion (Table 1).

Table 2. Release rates of sol-gels in this study and Pramik (2017) as flow tank tests progressed. Values in the bottom rows of each section are normalized to account for the different volume of sol-gel injected in the two tests.

	Cosgrove (2020)		
	2 Minutes	3 hours	21 hours
g/day	5.72	1.65	1.04
g/day/10 mL of sol-gel	1.43	0.41	0.26
	Pramik (2017)		
	7 Hours	13 Hours	28 Hours
g/day	1.56	0.05	0.001
g/day/10 mL of sol-gel	0.20	0.009	0.0002

This can be compared to Pramik (2017), which gives a linear flow velocity of 0.213 m/d, or 0.89 cm/hr, and has MnO₄⁻ last detected at the 10 mg/L level no more than 28 hours from pumping start 19 cm from the injection point. At that rate, an advection point travelling from the injection well over 28 hours would have travelled 25 cm. That

study recorded lower release rates early in the test (Table 2), and a longer low-concentration tail than the present study, detecting a concentration of 6.48 $\mu\text{g/d}$ at hour 338. This study halted measurement at 25 hours when concentrations fell to zero. Therefore, although the plume of high concentration MnO_4^- observed in Pramik (2017) was shorter than in the present study, the overall plume was longer, including a long, low-concentration tail.

This conclusion conflicts with data from column testing, in which sol-gel injection into saturated sand failed to produce a longer release duration than injection of KMnO_4 alone (Figure 16), but sol-gel injection into dry sand produced a glassy gel strong enough to prohibit water flow that released MnO_4^- for a long period (Figures 17 & 18). That result was anticipated by Gupta (2013), which cites Pothamkury (1995) in noting that the glassy state attained by a sol-gel after gelation in a dry environment permits less diffusion than the gel state formed in the presence of water. Although the placement of a pre-formed, glassy column of SRP-G into a well has its attraction, it would forfeit the potential benefits of injection of the sol-gel as a fluid. That is, although the latter scheme might produce a less robust gel, it would permit the establishment of a laterally widespread permanganate barrier by injection from a few wells, as opposed to the interrupted barrier that would be produced by the placement of pre-formed SRP-G even with the use of many closely-spaced wells. Therefore, the establishment of a solution that will reliably gel in a saturated environment remains preferred.

CHAPTER 6: CONCLUSION

As a widespread contaminant that can cause cancer, organ damage, and other negative health effects, trichloroethylene (TCE) is a good target for new remediation technologies. As a DNAPL, it can spread widely through an aquifer once introduced, resulting in a wide area that must be treated. An SRP-G with a long gelation time and release duration could first spread through an aquifer in the same manner as the original TCE contamination before releasing an oxidant to remove it from the groundwater. As such, a greater volume of an aquifer could be treated with a small number of injections, useful particularly in targeting the diffuse tail of a TCE plume.

This study sought to produce an SRP-G using a solution of colloidal silica, potassium permanganate (KMnO_4), and sodium hydroxide (NaOH). This solution begins as a fluid, then forms a silica gel in a reaction catalyzed by the KMnO_4 and hypothetically extended by the NaOH . Containing the KMnO_4 as a continuous liquid phase, the silica gel slowly releases MnO_4^- . Three hypotheses regarding this sol-gel were tested: that low temperatures would increase gelation time in saturated soils, that a high pH would increase gelation time in batch tests, and that the injection of KMnO_4 dissolved in distilled water into a depleted silica gel would extend MnO_4^- release duration beyond the injection of either the SRP-G or the KMnO_4 alone. In the testing of these hypotheses, the three general methods used were to mix small batches of solution in glass beakers and measure viscosity over time, to inject sol-gel into sand-filled columns, pump water through, and measure MnO_4^- concentrations, and to inject sol-gel into a small flow tank and monitor its spread.

Tests of the first hypothesis were able to affirm that low temperature does increase gelation time, which suggests that an injection of SRP-G could be followed by an injection of cold water to extend its reach through the aquifer before gelation. Further, tests of the second hypothesis did not show a clear relationship between pH and gelation time, but only a narrow pH range was tested (9.36 to 9.44), so that further testing on this question may be merited. Finally, tests of repeated injections were inconclusive, because gelation was not achieved when expected. In future testing, it is suggested that a greater KMnO_4 concentration be used for injection into saturated sandy media than the 26 g/L concentration used here.

REFERENCES

- Alexander, G.B., Heston, W.M., and Iler, R.K. The solubility of amorphous silica in water. *J. Phys. Chem.* 58, 453–455.
- Amiri, A., Øye, G., and Sjöblom, J. (2009). Influence of pH, high salinity and particle concentration on stability and rheological properties of aqueous suspensions of fumed silica. *Colloids and surfaces A: Physicochemical Engineering Aspects*, 349(1-3).
- Bergna, H.E. (1994). Colloid chemistry of silica. *The Colloid Chemistry of Silica*. American Chemical Society, 234, doi: 10.1021/ba-1994-0234.ch001
- Butrón, C., Axelsson, M., and Gustafson, G. Silica sol for rock grouting: Laboratory testing of strength, fracture behaviour and hydraulic conductivity. *Tunnel. Underground Space Technol.* 24, 603–607.
- Boyer, A., Wendy, F., and Runyan, R. (2000, January). Trichloroethylene inhibits development of embryonic heart valve precursors *in Vitro*. *Toxicological Sciences*, 53(1).
- Chang, Q., Cerneaux, S., Wang, X., Zhang, X., Wang, Y., and Zhou, J. (2015). Evidence of ZrO₂ sol-gel transition by gelation time and viscosity. *Journal of Sol-Gel Science and Technology*, 73: 208-214. doi: 10.1007/s10971-014-3516-0
- Chapman, S. and Parker, B. (2005). Plume persistence due to aquitard back diffusion following dense nonaqueous phase liquid source removal or isolation. *Water Resources Research*, 41(W12411), doi:10.1029/2005WR004
- Christenson, M., Kambhu, A., Reece, J., Comfort, S., and Brunner, L. (2016). A five-year performance review of field-scale, slow-release permanganate candles with recommendations for second-generation improvements. *Chemosphere*, 150, 239–247.
- Dale, V. (2006, December). A regional simulation to explore impacts of resource use and constraints. SERDP Conservation project 1259.
- Depasse, J. and Watillon, A. (1970). The stability of amorphous colloidal silica. *J. Coll. Interface Sci.* 33, 430–438.
- Franks, G.V. (2002). Zeta potentials and yield stresses of silica suspensions in concentrated monovalent electrolytes: isoelectric point shift and additional attraction. *J. Coll. Interface Sci.* 249, 44–51.
- Gupta, N. (2013). Development and characterization of controlled-release permanganate gel for groundwater remediation. MS Thesis, Ohio University. Athens, OH.

- Hastings, J. (2015). Optimization and analysis of a slow-release permanganate gel for groundwater remediation in porous and low-permeability media. MS Thesis, Ohio University. Athens, OH.
- Huling, S. and Pivetz, B. (2006). In-situ chemical oxidation. *Engineering Issue*.
- Iler, R. K. (1979). The chemistry of silica: solubility, polymerization, colloid and surface properties and biochemistry, John Wiley & Sons.
- ITRC (Interstate Technology, Regulatory Council). (2012). Integrated DNAPL site strategy technology/regulatory guidance ITRC integrated DNAPL site strategy team.
https://www.itrcweb.org/guidancedocuments/integrateddnaplstrategy_idssdoc/idss-1.pdf
- Khan, M., Kaphalia, B., Kanz, M., Ansari, G., and Prabhakar, B. (1995, September). Trichloroethene-induced autoimmune response in female 14 MRL +/+ mice. *Toxicology and Applied Pharmacology*, 134.
- Koch, J. and Nowak, W. (2015). Predicting DNAPL mass discharge and contaminated site longevity probabilities: Conceptual model and high-resolution stochastic simulation. *Water Resources Research*. Doi:10.1002/2014WR015478
- Kueper, B.H., Wealthall, G.P., Smith, J.W.N., Leharne, S.A., and Lerner, D.N. (2003). Environment Agency, Bristol.
- Lee, E.S. and Schwartz, F.W. (2007a). Characteristics and applications of controlled release KMnO₄ for groundwater remediation. *Chemosphere*, 66(11), 2058-2066. doi:10.1016/j.chemosphere.2006.09.093
- Lee, E.S. and Schwartz, F.W. (2007b). Characterization and optimization of long-term controlled release system for groundwater remediation: A generalized modeling approach. *Chemosphere*, 69(2), 247 – 253. doi:10.1016/j.chemosphere.2007.04.037
- Lee, E.S., Woo, N.C., Schwartz, F.W., Lee, B.S., Lee, K.C., Woo, M.H., Kim, J.H., and Kim, H.K. (2008). Characterization of controlled-release KMnO₄ (CRP) barrier system for groundwater remediation: A pilot-scale flow-tank study. *Chemosphere*, 71(5), 902-910. doi:10.1016/j.chemosphere.2007.11.037
- Lee, B.S., Kim, J.H., Lee, K.C., Kim, Y.B., Schwartz, F.W., Lee, E.S., Woo, N.C., and Lee, M.K. (2009). Efficacy of controlled-release KMnO₄ (CRP) for controlling dissolved TCE plume in groundwater: A large flow-tank study. *Chemosphere*, 74, 745-750.
- Lide, D. (Ed.) (2004, June). Handbook of chemistry and physics. CRC Press LLC.

- Mao, H., Wang, C., and Wang, K. (2014). Gelation performance of cationic gemini silica sol with inorganic salts and its antibacterial property analysis. *Journal of Dispersion Science and Technology*, 35:1208–1213.
- Mercer, J.W. and R.M. Cohen (1990). A review of immiscible fluids in the subsurface: Properties, models, characterization and remediation, *Journal of Contaminant Hydrology*, 6(2), 107–163.
- Murakata, T., Sato, S., Ohgawara, T., Watanabe, T., and Suzuki, T. (1992, March). Control of pore size distribution of silica gel through sol-gel process using inorganic salts and surfactants as additives. *Journal of Materials Science*, 27.
- Omoike, A.I. and Harmon, D. (2019). Slow-releasing permanganate ions from permanganate core-manganese oxide shell particles for the oxidative degradation of an algae odorant in water. *Chemosphere*, 223, 391–398.
<https://doiorg.proxy.library.ohio.edu/10.1016/j.chemosphere.2019.02.036>
- Pankow, J. and Cherry, J. (1996) Dense chlorinated solvents and other DNAPLs in groundwater: History, behaviour and remediation. Waterloo Press, Oregon.
- Pedrotti, M., Wong, C., El Mountassir, G., and Lunn, R.J. (2017). An analytical model for the control of silica grout penetration in natural groundwater systems. *Tunnelling and Underground Space Technology*, 70, 105-113.
- Pokusaev, B.G., Karlov, S.P., Vyaz, A.V., and Nekrasov, D.A. (2018). Laws of the formation and diffusion properties of silica and agarose gels. *Theoretical Foundations of Chemical Engineering*, 52(2), 222–233.
<https://doiorg.proxy.library.ohio.edu/10.1134/S0040579518020136>
- Pothamkury, U.R. and Barbosa-Canovas, G.V. (1995). Fundamental aspects of controlled release in foods. *Trends in Food Science & Technology*, v. 6, p. 397-406.
- Pramik, Paige. (2017). Optimization and analysis of a slow-release permanganate gel for dilute DNAPL plume remediation in groundwater. MS Thesis, Ohio University. Athens, OH.
- Radican, L., Wartenberg, D., Rhoads, G., Schneider, D., Wedeen, R. Stewart, P., and Blair, A. (2006). A retrospective occupational cohort study of endstage renal disease in aircraft workers exposed to trichloroethylene and other hydrocarbons. *Journal of Occupational and Environmental Medicine*, 48(1), 1-12.
- Rivett, M.O., Lerner, D.N., and Lloyd, J.W. (1990). Temporal variations of chlorinated solvents in abstraction wells. *Ground Water Monitoring Review*, 10(4), 127–133.

- Shim, W.S., Yoo, J.S., Bae, Y.H., and Lee, D.S. (2005). Novel injectable pH and temperature sensitive lock copolymer hydrogel. *Biomacromolecules*, 6, 2930-2934.
- Siahpoosh, S.M. (2011). Microstructure and gel kinetics in silica composite gels for application in mass transport research. MS Thesis. Chalmers University of Technology. Gothenburg, Sweden.
- Sögaard, C., Funehag, J., Gergorić, and Abbas, Z. (2018). The long term stability of silica nanoparticle gels in waters of different ionic compositions and pH values. *Colloids and Surfaces A*. 544, 127-136.
- Stroo, H.F. and Ward, C.H. (Eds.). (2010). In situ remediation of chlorinated solvent plumes. New York, NY: Springer Science + Business Media.
- Trompette, J.L. and Meireles, M. (2003). Ion-specific effect on the gelation kinetics of concentrated colloidal silica suspensions. *Journal of Colloid and Interface Science*, 263(2), 522-527.
- US EPA. (2001, August). Trichloroethylene health risk assessment: Synthesis and characterization. EPA/600/P-01/002A
- US EPA. (2002, January). Groundwater Remedies Selected at Superfund Sites. EPA-542-R-01022. Retrieved from https://www.epa.gov/sites/production/files/201504/documents/gw_remed_selected.pdf
- US EPA. (2003, December). The DNAPL remediation challenge: Is there a case for source depletion?
- US EPA. (2009). DNAPL remediation: Selected projects where regulatory closure goals have been achieved. EPA/542/R-09/008. www.cluin.org/download/remed/542r09008.pdf
- US EPA (2015, November 19). Contaminated site clean-up information: Dense nonaqueous phase liquids (DNAPLs). Retrieved from [https://clu.in.org/contaminantfocus/default.focus/sec/Dense_Nonaqueous_Phase_Liquids\(DNAPLs\)/cat/Overview/](https://clu.in.org/contaminantfocus/default.focus/sec/Dense_Nonaqueous_Phase_Liquids(DNAPLs)/cat/Overview/)
- US EPA (2016, February 5). Contaminated site clean-up information: Trichloroethylene (TCE). Retrieved from [https://clu.in.org/contaminantfocus/default.focus/sec/Trichloroethylene\(TCE\)/cat/Overview/](https://clu.in.org/contaminantfocus/default.focus/sec/Trichloroethylene(TCE)/cat/Overview/)
- Yan, Y. and Schwartz, F. (2000). Kinetics and mechanisms for TCE oxidation by permanganate. *Environmental Science & Technology*. 34(12), pp. 2535-2541.

APPENDIX A: BATCH TEST DATA

Table A1. Room temperature ($\sim 23^{\circ}\text{C}$) batch test with 26 g/L $[\text{KMnO}_4]$ and 140 mL of 45wt% colloidal silica. Times represented in 12-hour format.

Time	Hours	Viscosity (cP)
2:05	0.00	0
4:26	2.35	0
5:40	3.58	0
8:04	5.98	22600
9:13	7.13	17300

Table A2. Room temperature ($\sim 23^{\circ}\text{C}$) batch test with 26 g/L $[\text{KMnO}_4]$, 130 mL of 45wt% colloidal silica, and 10 mL of distilled water.

Time	Hours	Viscosity (cP)
2:32	0.00	0
4:29	1.95	0
8:08	5.60	600
9:17	6.75	60700

Table A3. Room temperature (23°C) batch test with 26 g/L $[\text{KMnO}_4]$, 120 mL of 45wt% colloidal silica, and 20 mL of distilled water. Times represented in 12-hour format.

Time	Hours	Viscosity (cP)
2:50	0.00	0
4:31	1.68	0
8:14	5.40	4600
9:19	6.48	58900

Table A4. Room temperature (23°C) batch test with 26 g/L [KMnO₄], 130 mL of 45wt% colloidal silica, and 10 mL of pH 12.43 NaOH solution. Times represented in 12-hour format.

Time	Hours	Viscosity (cP)
3:15	0.00	0
5:43	2.47	0
6:56	3.68	100
8:23	5.13	1200
9:45	6.50	26600
10:47	7.53	38500
12:17	9.03	36600

Table A5. Room temperature (23°C) batch test with 26 g/L [KMnO₄], 120 mL of 45wt% colloidal silica, and 20 mL of pH 12.43 NaOH solution. Times represented in 12-hour format.

Time	Hours	Viscosity (cP)
3:27	0.00	0
5:40	2.22	100
7:00	3.55	100
8:26	4.98	400
9:50	6.38	3100
10:51	7.40	16900
12:19	8.87	29900

Table A6. Chilled (2°C) batch test with 26 g/L [KMnO₄] and 140 mL of 45wt% colloidal silica. Times represented in 24-hour format.

Time	Hours	Viscosity (cP)
11:04	0.00	0
13:09	2.08	0
15:04	4.00	0
16:52	5.80	200
19:03	7.98	1200
20:11	9.12	4900
21:16	10.20	10700
21:57	10.88	19200
22:39	11.58	29300
0:37	13.55	45000
10:27	23.38	30200

Table A7. Chilled (2°C) batch test with 26 g/L [KMnO₄], 130 mL of 45wt% colloidal silica, and 10 mL distilled water. Times represented in 24-hour format.

Time	Hours	Viscosity (cP)
10:12	0.00	0
12:16	2.07	0
14:30	4.30	0
17:43	7.52	100
19:37	9.42	800
20:26	10.23	1700
21:49	11.62	4200
23:17	13.08	6400
1:04	13.87	19500
15:11	27.98	50700
20:25	33.22	65200

Table A8. Chilled (2°C) batch test with 26 g/L [KMnO₄], 120 mL of 45wt% colloidal silica, and 20 mL distilled water. Times represented in 24-hour format.

Time	Hours	Viscosity (cP)
11:11	0.00	0
13:52	2.68	0
16:26	5.25	0
18:49	7.63	0
19:48	8.62	100
21:15	10.07	100
23:35	12.40	200
3:19	16.13	2400
11:14	24.05	29100
12:40	25.48	30600
14:34	27.38	28200
16:35	29.40	30700
19:56	32.75	43400
23:22	36.18	0

Table A9. Chilled (2°C) batch test with 26 g/L [KMnO₄], 130 mL of 45wt% colloidal silica, and 10 mL of pH 12.43 NaOH solution. Times represented in 24-hour format.

Time	Hour	Viscosity (cP)
9:50	0.00	0
12:05	2.25	0
14:20	4.50	200
15:45	5.92	100
17:01	7.18	2900
18:32	8.70	7300
19:35	9.75	21000
20:41	10.85	21300
22:16	12.43	31300
0:12	14.37	34800
0:50	15.00	35000
11:13	24.38	47300

Table A10. Chilled (2°C) batch test with 26 g/L [KMnO₄], 120 mL of 45wt% colloidal silica, and 20 mL of pH 12.43 NaOH solution. Times represented in 24-hour format.

Time	Hours	Viscosity (cP)
11:23	0.00	0
13:55	2.53	0
16:23	5.00	100
18:47	7.40	0
19:46	8.38	100
21:19	9.93	100
23:31	12.13	100
3:27	16.07	700
12:00	24.62	4600
13:18	25.92	8400
14:31	27.13	15800
15:34	28.18	14400
16:32	29.15	20100
18:10	30.78	24100
19:53	32.50	26400
23:25	36.03	0

APPENDIX B: COLUMN TEST DATA

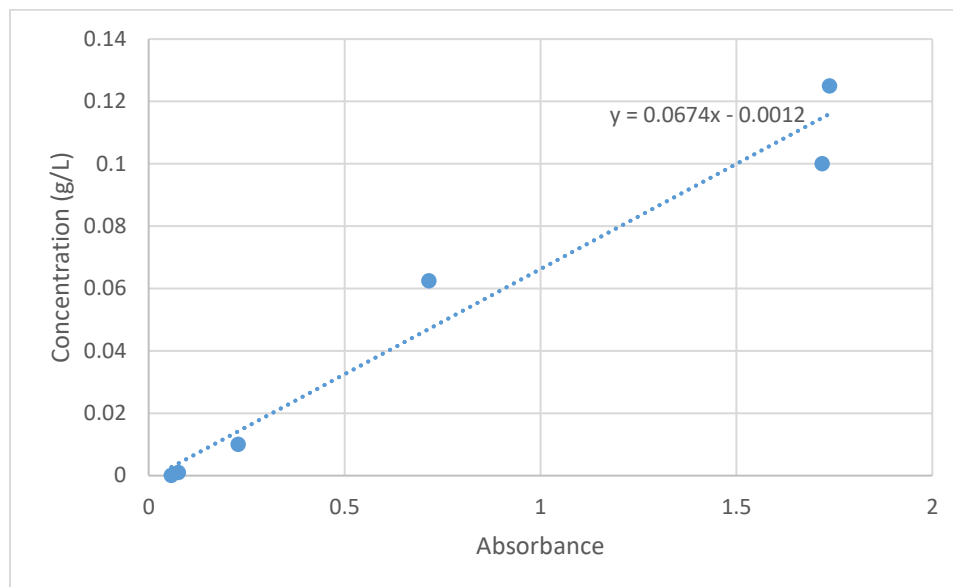


Figure B1. Curve used for conversion of absorbance values (at 454 nm wavelength) to MnO_4^- concentrations.

Table B1. MnO_4^- concentration following injection of 1 mL of 26 g/L $[\text{KMnO}_4]$ and 45 wt% colloidal silica sol-gel into a small glass column. No gelation time was allowed before pumping began.

Time	Minutes	Absorbance	Concentration (g/L)	Notes
11:15	0	0	0.00000	injection start
12:58	103	-0.017	0.00000	
13:24	129	-0.003	0.00000	plume reached end of column
14:52	216	1.643	0.10954	
16:05	289	1.055	0.06991	
18:00	404	-0.099	0.00000	
20:12	536	0.105	0.00588	

Table B2. MnO_4^- concentration following injection of 1 mL of 26 g/L $[\text{KMnO}_4]$ and 45 wt% colloidal silica sol-gel into a small glass column. Two days of gelation time was allowed before pumping began.

Date	Time	Minutes	Absorbance	Concentration (g/L)	Notes
15-Oct	17:13	0			injection start
	17:45	32	0.011	0.00	
	19:02	109	0.355	0.02	
	19:29	136			pause pump - allow for gelation
17-Oct	20:10				restart pumping
	20:27	153	0.337	0.02	
	21:33	216	0.286	0.02	
	23:10	313	0.232	0.01	
	0:30	393	0.172	0.01	

Table B3. Column test using 40 mL of sol-gel with 26 g/L $[\text{KMnO}_4]$ and 45 wt% colloidal silica. Flow rate 4.3 mL/min.

Pumping Status	Time	Minutes	Volume (mL)	Absorbance	Concentration (g/L)
On	11:32	0			
Off	11:47	15			
On	12:03	15	64	3.509	0.24
Off	12:13	25			
On	12:33	25			
On	12:56	48	206	3.402	0.23
Off	1:22	74			
On	5:10				
On	5:25	89	381	1.258	0.08
On	6:32	156	669	0.672	0.04
On	7:12	196	840	0.386	0.02
On	8:21	265	1136	0.157	0.01
Off	11:59	483	2070	0.028	0.00

Table B4. Column test using 40 mL of sol-gel with 40 g/L [KMnO₄] and 45 wt% colloidal silica. Flow rate 3.6 mL/min.

Pumping Status	Time	Minutes	Volume (mL)	Absorbance	Concentration (g/L)
On	11:32	0			
On	11:39	7	25	3.564	0.24
Off	11:47	15			
On	12:33				
Off	12:40	22			
On	12:47				
Off	1:22	57			
On	5:10				
On	5:25	72	257	3.378	0.23
On	6:00	107	382	2.547	0.17
On	7:09	176	629	0.084	0.00
On	8:21	248	886	0.02	0.00
Off	11:59	466	1664	0.004	0.00

Table B5. Column test using 40 mL of sol-gel with 50 g/L [KMnO₄] and 45 wt% colloidal silica. Flow rate 4.3 mL/min.

Pumping Status	Time	Minutes	Volume (mL)	Absorbance	Concentration (g/L)
On	11:32				
On	11:39	7	30	3.489	0.23
Off	11:47	15			
On	12:33				
On	12:55	37	159	3.36	0.23
On	1:07	49	210	3.34	0.22
On	1:22	64			
Off	5:10				
On	5:21	75	321	0.08	0.004
On	5:46	100	429	0.012	0.000
On	6:15	129	372	0.006	0.000
On	7:08	182	525	0.006	0.000
On	8:22	256	738	0.004	0.000
Off	11:59	473	1364	0.002	0.000

Table B6. Column test using 40 mL of sol-gel with 50 g/L [KMnO₄] and 50 wt% colloidal silica. Flow rate 2.9 mL/min.

Pumping Status	Time	Minutes	Volume (mL)	Absorbance	Concentration (g/L)
On	11:32				
Off	11:39	7	20	3.536	0.24
On	12:33				
On	12:55	29	84	3.402	0.23
On	1:13	47	136	3.307	0.22
Off	1:22	56			
On	5:10				
On	5:30	76	219	3.336	0.22
On	6:33	139	401	2.031	0.14
On	7:09	175	505	1.361	0.09
On	8:22	248	715	0.854	0.06
On	11:59	565	1630	3.336	0.22
Off	10:53	1941	5599	0.195	0.01

Table B7. First 10 mL injection of sol-gel with 26 g/L [KMnO₄] and 45 wt% colloidal silica prior reinjection test. Pumping of distilled water immediately followed injection at 3.8 mL/s.

Date	Time	Minutes	Volume (mL)	Absorbance	Concentration (g/L)	Release Rate (mg/min)
15-Jan	16:19	7	27	0.007	0.00	0.0000
	16:27	15	57	0.471	0.03	0.0070
	16:31	21	80	3.249	0.22	0.0497
	16:48	38	145	3.425	0.23	0.0524
	17:13	63	240	3.331	0.22	0.0510
	17:51	101	384	2.984	0.20	0.0456
	21:17	307	1168	0.288	0.02	0.0042
	22:41	391	1487	0.161	0.01	0.0022
16-Jan	0:05	475	1806	0.095	0.01	0.0012
	9:00	830	3156	0.09	0.005	0.0011
	9:13	843	3206	0.003	-0.0010	0.0000
	10:30	920	3499	0	-0.0012	0.0000

Table B8. Second 10 mL injection of sol-gel with 26 g/L [KMnO₄] and 45 wt% colloidal silica prior reinjection test. Pumping of distilled water followed 6 days after injection at 4.0 mL/s.

Date	Time	Minutes	Volume (mL)	Absorbance	Concentration (g/L)	Release Rate (mg/min)
22-Jan	4:39	0	0			
	4:54	15	60	3.44	0.23	0.0552
	5:22	43	171	3.44	0.23	0.0552
	9:16	277	1104	0.074	0.00379	0.0009
	10:06	327	1304	0.051	0.00224	0.0005
	11:15	378	1507	0.034	0.00109	0.0003
23-Jan	12:09	432	1722	0.028	0.00069	0.0002
	2:48	591	2356	0.018	0.00001	0.0000
	10:08	1031	4110	0.011	-0.00046	0
	2:46	1309	5219	0.004	-0.00093	0
	5:23	1466	5845	0.004	-0.00093	0
	9:13	1696	6761	0.005	-0.00086	0

Table B9. First 10 mL injection of 26 g/L [KMnO₄] solution. Pumping of distilled water followed immediately after injection at 2.8 mL/s.

Time	Minutes	Volume (mL)	Absorbance	Concentration (g/L)	Release Rate (mg/min)
5:03	0	0	0.0027		
5:06	3	8	3.439	0.23	0.0390
5:22	19	54	3.466	0.23	0.0393
5:35	32	90	3.385	0.23	0.0384
5:53	50	141	0.842	0.06	0.0094
6:05	62	175	0.467	0.03	0.0051
6:18	75	211	0.27	0.02	0.0029
6:33	90	254	0.155	0.01	0.0016
7:01	118	332	0.06	0.00	0.0005
7:41	158	445	0.025	0.00	0.0001

Table B10. Second 10 mL injection of 26 g/L [KMnO₄] solution. Pumping of distilled water followed immediately after injection at 4.1 mL/s.

Time	Minutes	Volume (mL)	Absorbance	Concentration (g/L)	Release Rate (mg/min)
11:46	0	0	3.505	0.24	0.0572
11:56	10	41	3.451	0.23	0.0563
12:20	34	138	0.814	0.05	0.0131
12:25	39	158	0.411	0.03	0.0064
12:31	46	186	0.195	0.01	0.0029
12:46	61	247	0.107	0.01	0.0015
1:14	89	361	0.074	0.00	0.0009
2:24	99	401	0.062	0.00	0.0007

APPENDIX C: FLOW TANK TEST DATA

Table C1. MnO_4^- concentrations measured in first row of flow tank monitoring wells. Refer to Figure 10 for placement of wells.

		Sample Well					
		Concentration (g/L)					
Date	Time	1	2	3	4	5	6
2-19	23:46			0.00032			

Table C2. MnO_4^- concentrations measured in second row of flow tank monitoring wells. Refer to Figure 10 for placement of wells.

		Sample Well					
		Concentration (g/L)					
Date	Time	11	12	13	14	15	16
2-19	16:52			0.5838			
	20:05			0.1683			
2-20	13:54			0.0106			
	18:05	0.0146					

Table C3. MnO_4^- concentrations measured in third row of flow tank monitoring wells. Refer to Figure 10 for placement of wells.

		Sample Well					
		Concentration (g/L)					
Date	Time	21	22	23	24	25	26
2-19	17:09				0.0030		
	17:13			0.0076			
	18:00				0.0055		
	19:48				0.0071		
	23:22				0.0374		
2-20	13:48				0.0091		

Table C4. MnO_4^- concentrations measured in fourth row of flow tank monitoring wells. Refer to Figure 10 for placement of wells.

		Sample Well					
		Concentration (g/L)					
Date	Time	31	32	33	34	35	36
2-19	17:00			0.0000			
	23:35			0.0246			
	23:38	0.0355					
	23:40					0.0050	
2-20	13:51			0.0113			
	14:39			0.0084			
	17:45			0.0087			
	17:48	0.0087					
	17:53					0.0231	



OHIO
UNIVERSITY

Thesis and Dissertation Services